

# BIOMECHANICAL ANALYSIS OF ABNORMAL CANINE AND AVIAN STIFLES

by

KATHERINE MCDOWELL BAKER

(Under the Direction of Timothy Foutz)

## ABSTRACT

By continuously measuring the kinematics of the stifle in all six degrees of freedom, the effects of various treatments may be quantitatively investigated. The Oxford knee rig provides a validated method of simulating deep flexion of the stifle *in vitro* while retaining its full range of motion and minimizing variability between animals. The studies herein used a modified Oxford knee rig and a three-dimensional motion capture system to investigate (i) the effects of tibial plateau angle and spacer thickness on canine total knee replacement and (ii) the variability of stifle kinematics among broiler chicken breeds with varying susceptibilities to leg deformities. Strain to the collateral ligaments in the canine and the gastrocnemius tendon in the broiler were also investigated. Results from both studies showed measurable changes in stifle kinematics, and results may be used to improve the welfare of canines with stifle osteoarthritis and chickens bred for rapid growth rate.

INDEX WORDS: Biomechanics, Oxford knee rig, Canine stifle, Total knee replacement, Tibial plateau angle, Cranial cruciate ligament, Collateral ligaments, Commercial broiler, Leg deformity, Gastrocnemius tendon

BIOMECHANICAL ANALYSIS OF ABNORMAL CANINE AND AVIAN STIFLES

by

KATHERINE MCDOWELL BAKER

B.S., GEORGIA INSTITUTE OF TECHNOLOGY, 2011

A Thesis Submitted to the Graduate Faculty of The University of Georgia in Partial Fulfillment of the  
Requirements for the Degree

MASTER OF SCIENCE

ATHENS, GEORGIA

2013

© 2013

Katherine McDowell Baker

All Rights Reserved

BIOMECHANICAL ANALYSIS OF ABNORMAL CANINE AND AVIAN STIFLES

by

KATHERINE MCDOWELL BAKER

Major Professor: Timothy Foutz

Committee: Steven Budsberg  
Kyle Johnsen

Electronic Version Approved:

Maureen Grasso  
Dean of the Graduate School  
The University of Georgia  
May 2013

## DEDICATION

I dedicate this work to my dog-loving family who encouraged me to get a master's degree, have patiently supported me the last two years, and were always interested in what I was doing in lab even when it was a little gory. Thank you.

## ACKNOWLEDGEMENTS

I would like to express my appreciation to my major professor, Dr. Tim Foutz, for his continual support over the last two years and for allowing me the independence to pursue my own research interests while still guiding me in the right direction. I am thankful to my committee members Dr. Kyle Johnsen for reviewing this manuscript, and Dr. Steve Budsberg for putting in the time to perform so many TKR's on cadaver legs and having such a good sense of humor about it. I would like to acknowledge Dr. Sammy Aggrey from the Poultry Science department for supplying the chickens, and BioMedtrix for providing the custom TKR implants.

I would also like to thank my lab partner, Andy Rodgers, who built the OKR and saved me from boredom in lab on a daily basis. Finally, I would like to thank Megan Hansen and Bryan Torres, who were always willing to go above and beyond to help my project from procuring and cutting up legs to helping me navigate the vet school. It was a pleasure to work with everyone mentioned. Thank you.

## TABLE OF CONTENTS

|  | Page |
|--|------|
| ACKNOWLEDGEMENTS.....  | v    |
| CHAPTER  |      |
| 1 INTRODUCTION.....  | 1    |
| 2 IN VITRO EFFECTS OF TIBIAL PLATAU ANGLE AND SPACER THICKNESS ON CANINE TOTAL KNEE<br>REPLACEMENT ..... | 2    |
| 2.1 Abstract .....   | 3    |
| 2.2 Introduction and Literature Review .....   | 4    |
| 2.3 Purpose of Study .....   | 14   |
| 2.4 Materials and Methods .....  | 14   |
| 2.5 Results .....  | 21   |
| 2.6 Discussion .....   | 32   |
| 2.7 Conclusion .....   | 34   |
| 2.8 References.....  | 36   |
| 3 IN VITRO KINEMATICS OF THE STIFLE AND GASTROCNEMIUS TENDON STRAIN IN THREE CHICKEN<br>BREEDS.....      | 39   |
| 3.1 Abstract .....   | 40   |
| 3.2 Introduction and Literature Review .....   | 41   |
| 3.3 Purpose of Study .....   | 48   |
| 3.4 Materials and Methods .....  | 49   |

|                                  |    |
|----------------------------------|----|
| 3.5 Results .....                | 53 |
| 3.6 Discussion .....             | 62 |
| 3.7 Conclusion .....             | 64 |
| 3.8 References .....             | 65 |
| 4 SUMMARY & CONCLUSION.....      | 68 |
| 4.1 Summary.....                 | 68 |
| 4.2 Future Recommendations ..... | 69 |

## CHAPTER 1

### INTRODUCTION

Movement of the animal stifle requires complex interactions between the various structures of the joint and is best assessed through an objective technique known as three-dimensional (3-D) kinematic analysis. *In vivo* kinematic analysis typically involves walking an animal through a known control region and monitoring the position of key anatomical locations via an imaging system. The 3-D relationship of the joint's bone segments are used to quantify joint angles and translations. *In vitro* kinematic analysis involves cadaver stifles which are mechanically moved through a series of positions, and the 3-D relationships of the joint segments are again quantified as angulations and translations. One common method of generating this mechanical movement of the cadaver stifle is an Oxford Knee Rig (OKR). The OKR is a proven method of simulating deep flexion in the cadaver stifle while allowing for all six degrees of freedom of the joint. The OKR provides a way to test stifle joints *in vitro*, minimizing variability between subjects and allowing comparison of multiple variables within a subject.

The objective of the two studies presented herein is to assess the stifle kinematics of two animals that have a history of biomechanical problems at the stifle joint. The first study compares the kinematics of the normal canine stifle to an artificial stifle with varying tibial plateau angles. The second study compares the kinematics of the broiler stifle from birds with various ranges of leg deformities and lameness. The results from both studies may lead to improvements in veterinary practices which may increase the quality of life for both canines and commercial chickens.

## CHAPTER 2

### In Vitro Effects of Tibial Plateau Angle and Spacer Thickness on Canine Total Knee Replacement <sup>1</sup>

---

<sup>1</sup> Baker, K.B., T.L. Foutz, K.J. Johnsen, and , S.C. Budsberg. To be submitted to the *American Journal of Veterinary Research*.

## 2.1 Abstract

**Objective-** To quantify the *in vitro* three-dimensional kinematics and collateral ligament strain of the canine stifle before and after cranial cruciate ligament (CrCL) transection followed by total knee replacement (TKR) with varying tibial plateau angles and spacer thicknesses.

**Sample-** Six hemi-pelvises collected from non-chondrodystrophic canines, ranging between 25 and 35 kg, euthanized for reasons unrelated to this study.

**Procedure-** Each hemi-pelvis was mounted on a modified Oxford knee rig that allowed for all six degrees of freedom of the stifle while preserving the hip and hock joints. Stifles were flexed from 140° extension to 90° flexion while kinematic data and strain to the collateral ligaments were measured continuously. Data was again collected after CrCL transection and TKR with combinations of three tibial plateau angles (8, 4, 0 degrees) and 3 spacer thicknesses (5, 7, 9 mm). Joint coordinate systems on the femur and tibia were constructed to calculate stifle kinematics in all six degrees of freedom.

**Results-** Normal stifle rotations were comparable to those previously found *in vivo*. The 8 degree 5 mm implant resulted in kinematics closest to the normal stifle. Decreasing the plateau angle caused a reversal in kinematics to abduction, external rotation, and lateral translation. Increasing spacer thickness caused a decrease in adduction and reversals to external rotation and lateral translation. Strain to the medial collateral ligament was minimal in the normal stifle and was not affected by TKR. Peak strain to the lateral collateral ligament was 5.7% in the normal stifle, which decreased with steeper plateau angles but returned to normal with the 0 degree implant.

**Conclusions-** The steeper 8 degree implant paired with the 5 mm spacer used in this study restored the kinematics most closely to the normal stifle. Both decreasing plateau angle and increasing spacer thickness negatively affected stifle kinematics. Further studies on the tibial plateau angle in canine TKR's should investigate angles greater than 8 degrees to determine the possible benefits of steeper tibial plateau angles on kinematics and collateral ligament strain.

Table 2.1: List of Abbreviations.

|      |                                   |
|------|-----------------------------------|
| CaCL | Caudal cruciate ligament          |
| CrCL | Cranial cruciate ligament         |
| OKR  | Oxford knee rig                   |
| LCL  | Lateral collateral ligament       |
| MCL  | Medial collateral ligament        |
| TKR  | Total knee replacement            |
| TPA  | Tibial plateau angle              |
| TPLO | Tibial plateau leveling osteotomy |

## 2.2 Introduction and Literature Review

### 2.2.1 Background and Importance

Cranial cruciate ligament deficiency is the leading cause of stifle osteoarthritis in canines.<sup>1-3</sup> In 2003, the annual economic impact related to this condition was estimated to be \$1.32 billion in the United States alone.<sup>4</sup> The reported prevalence of CrCL deficiency has more than doubled over the last 30 years due to longer life expectancies in canines and improved diagnosis of the joint condition.<sup>5</sup> In some canines with CrCL disease, progression of osteoarthritis occurs even after stabilization or reconstructive surgery. For canines with failed prior surgical procedures or severe stifle osteoarthritis, total knee replacement, a more invasive surgical procedure, may be required to restore the function of the joint.<sup>6</sup> TKR has been performed on canines in the research setting for many years; however, the first commercial canine TKR for osteoarthritis was performed in 2005 with only 50 procedures completed by 2008.<sup>6,7</sup> So far, TKR in canines has been shown to improve postoperative joint function, but as of yet, full function of the stifle after TKR has not been achieved.

### 2.2.2 Stifle Anatomy and CrCL Deficiency

The cruciate ligaments of the canine stifle, the CrCL and the caudal cruciate ligament (CaCL), originate within the distal femoral intercondylar notch and attach to the intercondylar area of the tibia (Figure 2.1). These ligaments provide primary support for craniocaudal and axial stability of the stifle. The CrCL functions to limit excess cranial tibial displacement, internal tibial rotation, and hyperextension

of the stifle. In contrast, the CaCL prevents excess caudal tibial displacement and limits excess internal tibial rotation. While CrCL rupture can occur due to trauma, typically cruciate disease progresses slowly under normal loading, and diagnosis is not made until severe rupture.<sup>3</sup> Rupture of the CrCL causes stifle joint instability and abnormal joint motions that can damage surrounding cartilage and tissues. Previous studies indicate that both cranial tibial thrust and internal tibial rotation increase immediately after transection of the CrCL and fail to improve over time. Tashman et al.<sup>8</sup> suggests that cranial tibial thrust continues to increase and become more abnormal over time with the largest changes occurring between 6 and 12 months after transection. It was hypothesized that further progression of osteoarthritis after CrCL rupture may be due to overload failure of the meniscus. CrCL transection has been shown to lead to meniscal fibrillation and tears in at least 85% of dogs after 48 weeks.<sup>9</sup> While the relationship between excess tibial thrust and osteoarthritis are still under investigation, it is assumed that there is a direct correlation between the amount of excess tibial thrust after CrCL injury and the progression of osteoarthritis within the canine stifle.<sup>8,10,11</sup>

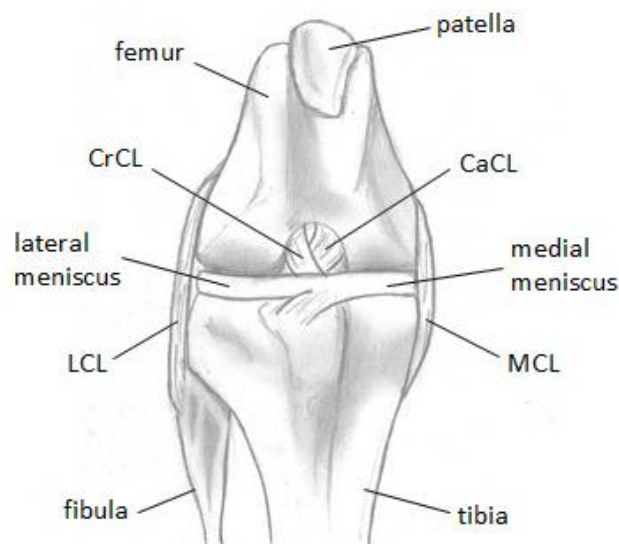


Figure 2.1: Illustration of canine stifle anatomy showing the femur, patella, cranial cruciate ligament (CrCL), caudal cruciate ligament (CaCL), lateral meniscus, medial meniscus, lateral collateral ligament (LCL), medial collateral ligament (MCL), fibula and tibia.

The tibial plateau angle (TPA) is a measure of the angle of the articulating surface of the tibia and the femur. It is typically measured from preoperative radiographs as the angle between (a) the long axis of the femur drawn from the midpoint of the intercondylar eminences to the center of the tarsal joint; and (b) the medial tibial plateau drawn from the proximal tibia's most cranial to caudal radiographic margins (Figure 2.2).<sup>12</sup> Although the natural canine tibial plateau angle is approximately 24°, implants are currently being inserted at 6° in an effort to minimize excess cranial tibial thrust that occurs due to the ruptured ligament.<sup>6</sup> No studies were found investigating the effects of tibial plateau angle on canine TKR.



Figure 2.2: Radiograph of the canine stifle (A) preoperatively with a naturally steep tibial plateau angle and (B) postoperatively with a flattened tibial plateau angle.

### 2.2.3 Current Solutions

Due to the high prevalence of CrCL injury in canines, there are multiple corrective procedures currently used to treat CrCL rupture in canines in an attempt to restore joint function. However, since no procedure has been proven superior in terms of functional outcome or complication rates, the course of

treatment for CrCL deficiency is typically based on the severity of the condition and surgeon preference.<sup>13,14</sup> Extracapsular Stabilization is a method that uses a non-absorbable suture pattern around the lateral fabella and the tibial crest to mimic the function of the CrCL. This technique is often unsuitable for large breed dogs as the suture is more likely to stretch or rupture.<sup>14,15</sup> Both Tibial Tuberosity Advancement and Fibular Head Transposition involve altering the position of alternate ligaments of the stifle to stabilize the joint. During Tibial Tuberosity Advancement, the tibial tuberosity is moved forward using a metal spacer and screws to realign the patellar ligament to counteract excess cranial tibial thrust.<sup>16,17</sup> Fibular Head Transposition uses the lateral collateral ligament to stabilize the joint.<sup>18,19</sup>

Plateau leveling techniques, including Cranial Wedge Osteotomy and Tibial Plateau Leveling Osteotomy (TPLO), decrease the tibial plateau angle, effectively mitigating cranial tibial thrust and eliminating the need for the CrCL in the craniocaudal plane.<sup>20</sup> TPLO is thought to be the most popular treatment for CrCL deficiency in medium to large breed dogs; however, it has been shown that further progression of osteoarthritis is present in at least 10% of dogs after treatment.<sup>21</sup> An *in vitro* study by Kim and Pozzi<sup>21</sup> suggests that TPLO restores the proper canine joint alignment during weight bearing but does not restore normal patterns of load distribution across the articulating surfaces of the joint. It is hypothesized that these abnormal loads cause excess wear on the menisci. Reports of complication rates for these procedures requiring further medical treatment vary widely among studies and range from 12-59% (Table 2.2).

Table 2.2: Complication Rates of Procedures Used to Treat CrCL Deficiency.

| Procedure                         | Complication Rate            |
|-----------------------------------|------------------------------|
| Extracapsular Stabilization       | 12.5-21% <sup>14</sup>       |
| Tibial Tuberosity Advancement     | 31.5-59% <sup>16,17</sup>    |
| Fibular Head Transposition        | 16.7-25.7% <sup>18,19</sup>  |
| Cranial Wedge Osteotomy           | 28% <sup>20</sup>            |
| Tibial Plateau Leveling Osteotomy | 17.4-28% <sup>14,22-24</sup> |

#### 2.2.4 Total Knee Replacement

Despite the many procedures available to treat CrCL deficiency, in many canines the progression of osteoarthritis continues even after corrective procedures until the joint is dysfunctional. The aim of TKR is to recover the natural joint function of the stifle by restoring mobility and stability without the presence of the CrCL once other surgical procedures have failed. The first canine total knee replacement became commercially available in 2005 and is comprised of two components: a cobalt-chrome femoral component and an ultrahigh molecular weight polyethylene tibial component.<sup>6</sup> During the procedure, the joint capsule is incised proximally, and both cruciate ligaments and menisci are excised. Osteotomies are performed on the proximal end of the tibia and the distal end of the femur at angles predetermined by cutting blocks used during surgery.<sup>6,7</sup>

Both implant components are available in varying widths, determined by superimposing sizing templates over preoperative radiographs of the joint. The tibial component is also available in varying thicknesses from 5 to 9 mm to fill the joint gap created by the osteotomies. Problems can occur if an inappropriate tibial component thickness is chosen because an excess joint gap may cause a deficient amount of contact between the articulating surfaces leading to joint instability, while over stuffing may cause excess strain on the collateral ligaments. While the correct tibial spacer thickness is also determined from preoperative radiographs, any deviation of the location of the tibial cut during surgery may change the spacer thickness needed to stabilize the joint. Therefore, it is often up to the surgeon to test and adjust the spacer thickness during the procedure and rely on the feel of the joint in passive flexion and extension during surgery. Neither the reliability of the surgeon in determining tibial spacer thickness during surgery, nor its effects on joint stability is well documented in canine TKR's.

The angle at which the tibial osteotomy is performed determines the stifle's new plateau angle. A CrCL-deficient stifle undergoes excess cranial tibial thrust because the ligament can no longer counteract the effects of the natural 24° angle of the tibial plateau. Liska and Doyle<sup>6</sup> anticipated that the optimal

TPA for canine knee replacements would be approximately 6°. This angle was based on a study performed by Warzee et al.<sup>25</sup> involving TPLO procedures; therefore, canine knee replacements are currently implanted with a 6° posterior tibial slope. During the less invasive TPLO procedure, a radial osteotomy is performed on the proximal tibia, and the tibial plateau is rotated to achieve the desired TPA of approximately 6°. The damaged CrCL is typically removed during surgery; however, the CaCL remains intact assuming no damage to the ligament.<sup>21,26</sup> The aim of the TPLO procedure is to decrease the tibial slope from 24° to 6°, which converts cranial tibial thrust to caudal tibial thrust. Since the CaCL is still intact, it prevents excess caudal tibial thrust.<sup>25,26</sup>

When comparing TPLO and TKR procedures, it is critical to note that the CaCL remains intact during a TPLO but is removed during a canine TKR. Therefore, the 6° TPA that has been shown to be optimal in TPLO procedures may not be optimal for TKR procedures. This drastically decreased angle is expected to cause excess caudal tibial thrust following a TKR procedure because the CaCL is not intact to prevent the excess caudal tibial movement. It is understood that abnormal tibial thrust causes progressive damage to the surrounding ligaments and implant components.<sup>21</sup> Therefore, varying the plateau angle in canine TKR should lead to varying degrees of craniocaudal tibial thrust and influence the kinematics of the joint as well as the success of the procedure. No studies were found investigating tibial plateau angle in canine TKR.

#### 2.2.5 Tibial Plateau Angle in Human TKR

While limited data is available on the effects of TPA on the outcome of TKR in canines, data is available on the human knee to support the hypothesis that tibial plateau angle has quantifiable effects on the kinematics of the stifle. In contrast to the canine stifle, the natural TPA in human knees ranges from approximately 10 to 15 degrees.<sup>27,28</sup> In a study by Bellemans et al.,<sup>29</sup> twenty-one human cadaveric legs were implanted with knee replacements with tibial slopes from 0-7°. Maximal flexion was tested postoperatively, and an average gain of 1.7° of flexion for every degree of extra tibial slope was found.

Ostermeier et al.<sup>30</sup> performed an *in vitro* study on seven legs undergoing TKR to determine the amount of quadriceps force required to extend the leg with surgical TPA's of 0° and 10°. Results suggested that steeper tibial slope results in a more physiologic movement and requires less quadriceps force during flexion and extension. Finally, Malviya et al.<sup>31</sup> investigated range of knee flexion based on multiple factors including tibial slope. For 101 TKR patients, a moderate correlation (R=0.58) was found between 12-month postoperative range of motion and TPA. This study also reported that range of motion increased by 2.6° for every degree of tibial slope. These studies suggest that varying the TPA during TKR in humans causes a change in the kinematic motions of the knee joint and that increasing tibial slope leads to greater degrees of extension and mobility. However, with an excessively large TPA, the posterior lip of the tibia may not be able to prevent anterior subluxation of the tibial component.<sup>29</sup>

#### 2.2.6 The Oxford Knee Rig

The kinematics of the human knee have been researched extensively both *in vitro* and *in vivo* to map its natural motions in an effort to replicate the motions of a healthy knee. *In vivo* studies more fully represent physiological conditions, which are impossible to replicate fully with cadaveric studies. However, an advantage to *in vitro* systems is that test conditions are more easily altered and evaluated within specimens, minimizing variability among specimens.<sup>32</sup> To simulate the natural kinematic motions of the stifle in a cadaveric hind limb, the joint must travel through all six degrees of freedom clinically described as three rotations (flexion/extension, adduction/abduction, internal/external) and three translations (cranial/caudal, medial/lateral, proximal/distal) shown in Figure 2.3. The Oxford knee rig (OKR) was first designed by Bourne et al.<sup>33</sup> for the simulation of knee kinematics in human cadaveric specimens and has been shown to allow all six degrees of freedom of the knee. Subsequent studies using canine cadaver models to investigate corrective surgical techniques for CrCL injuries typically involved removing all musculature from the specimen. Additionally, previous rigs typically have simulated the gait only at the midpoint of the stance phase, and limited kinematic data is collected with

a focus on craniocaudal translation and axial rotation. Results have varied significantly and are difficult to compare with *in vivo* literature.

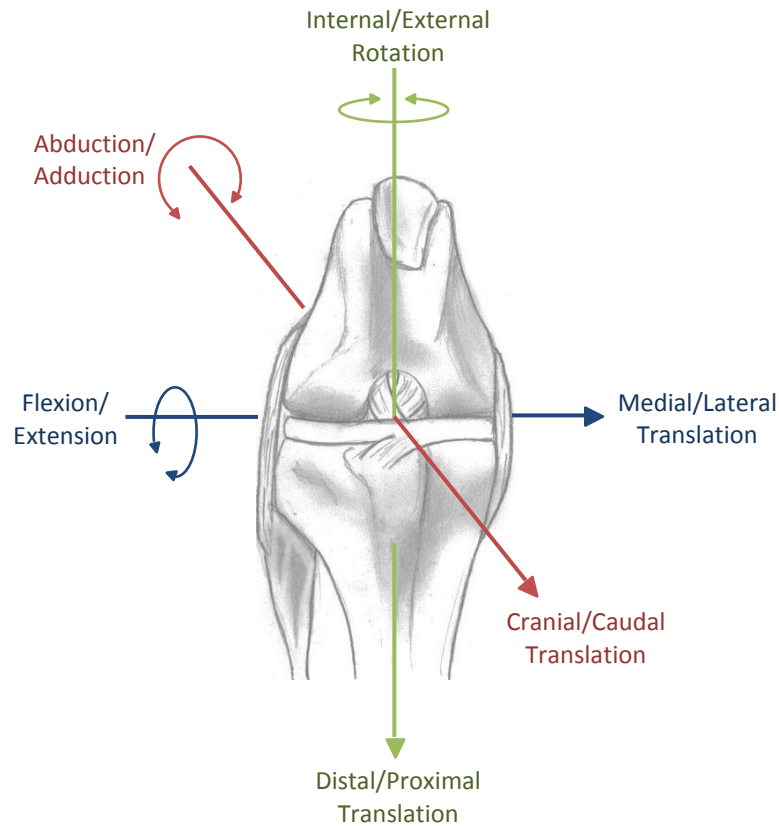


Figure 2.3: The six degrees of freedom of the stifle are clinically described as three rotations (flexion/extension, internal/external, adduction/abduction) and three translations (cranial/caudal, medial/lateral, proximal/distal).

Warzee et al.<sup>25</sup> oriented canine cadaveric specimens with the tarsal joint intact on a loading frame at the midpoint of the stance phase of a walk and simulated gastrocnemius and quadriceps muscle forces. Kinematic data collected included craniocaudal translation and axial rotation as determined from lateral radiographs. Results indicated that CrCL transection caused 19 mm cranial tibial thrust while TPLO caused 6 mm caudal tibial thrust with respect to the normal stifle. CrCL transection resulted in an

internal rotation of 23°, and the subsequent TPLO significantly decreased but did not entirely eliminate internal rotation to 10° compared to the normal stifle.

Reif et al.<sup>26</sup> mounted specimens onto a custom rig at an angle corresponding to the position of the stifle during weight bearing with the tibial plateau mounted onto a circular frame to simulate a radial osteotomy at varying degrees. Specimens were placed under a series of loads while cranial tibial translation was induced by a constant cranial pull on the tibial crest. The distal portion of the testing device was connected to a universal joint to simulate the tarsal joint. Craniocaudal translation was the only kinematic variable reported and was measured with a potentiometer. Results indicated that CrCL transection caused 14 mm cranial tibial thrust with respect to the normal stifle, and TPLO caused 2 mm caudal tibial thrust.

Chailleux et al.<sup>34</sup> prepared specimens by transecting the proximal end of the femur and the distal end of the tibia and potting both ends for fixation. The femur was attached to a testing apparatus with a bearing mechanism allowing axial rotation and translations to simulate the hip while the tibial end was left free. Motion was dynamically induced by a force on the quadriceps tendon throughout a flexion range of 90° to 30°. Craniocaudal translation and two rotations were measured with an electromagnetic tracking system. Unlike previous studies, results indicated that CrCL transection had no significant impact on craniocaudal translation compared to the normal stifle, and the subsequent TPLO caused approximately 11 mm caudal tibial thrust over the range of motion. After CrCL transection, axial rotation and adduction showed no significant differences from the normal stifle. However, after TPLO both external rotation and adduction significantly increased by approximately 8° and 5° respectively.

Kim et al.<sup>21</sup> prepared specimens by preserving the tarsal and stifle joint capsules and simulating gastrocnemius and quadriceps muscle forces. Specimens were mounted to a custom femoral jig mounted on a materials testing machine allowing for adjustment of the hip. During static loading with the stifle at the midpoint of the stance phase of a walk, only axial rotation of the femoral component

was unconstrained. Nylon screws implanted in the tibia and femur were landmarks for static positions of the stifle joint. Results indicated that CrCL transection increased cranial tibial thrust by 15 mm and internal tibial rotation by 14°, and the subsequent TPLO restored normal craniocaudal translation and axial rotation.

While many of these studies used the OKR to drive the motion of the cadaveric specimen with little to no muscle retained, it has been suggested that such techniques may cause distortion of the joint's natural motions due to a loss of the muscle tensions and constraints placed across the joint. Varadarajan et al.<sup>32</sup> suggests that the inclusion of muscle provides more physiologic constraints and has important implications with regard to the ability of OKR setups to simulate physiologic knee motion. Wilson et al.<sup>35</sup> found that in human cadaveric knees flexed passively without simulating muscle forces, internal rotation, abduction, and all three components of translation are coupled to flexion/extension angle in the normal knee.

It has been suggested that by retaining the soft tissue around the joint as well as the adjacent tarsal joint, cadaveric studies may more accurately simulate *in vivo* joint kinematics.<sup>32</sup> Currently limited canine stifle kinematic data is available from previous studies that mainly focus on craniocaudal translation and axial rotation. To fully determine the effects of any surgical procedure on a CrCL transected stifle, all six degrees of freedom of the joint should be investigated, as treatments may cause significant changes in other motions besides cranial translation and internal rotation. The majority of studies found have limited their investigation to effects of a treatment during a static pose at the midpoint of the stance phase. The kinematics of the stifle change during the gait cycle; therefore, it would be ideal to investigate the kinematics continuously throughout a full gait cycle. In order to obtain complete kinematic data over the full gait, a method of data collection that is capable of continuously measuring all six rotations and translations of the stifle should be investigated. By preserving the surrounding

musculature and collecting data over a full motion cycle, results may be more comparable to results from *in vivo* literature.

### 2.3 Purpose of Study

The primary purpose of this study was to characterize the kinematic motion of the canine cadaver stifle before and after TKR at varying tibial plateau angles paired with varying tibial spacer thicknesses. A secondary objective was to determine the effects of both plateau angle and spacer thickness on strain to the collateral ligaments as excess strain to these tissues could cause further damage to the already vulnerable joint. The questions of interest were: was there significant variability in kinematics and ligament strain between TKR trials implanted (1) at varying tibial plateau angles; and (2) with varying tibial spacer thicknesses.

Understanding how joint motions change after manipulation of these two tibial component variables will provide valuable information on how varying TKR components alters the mechanical properties of the stifle joint postoperatively. This will provide an essential basis for improvements to and optimization of the current canine TKR implant design, leading to greater postoperative success rates and a quality of life for canines impacted by stifle osteoarthritis.

### 2.4 Materials & Methods

#### 2.4.1 Specimen Preparation

Six hemi-pelvises were collected from non-chondrodystrophic canines ranging between 25 and 35 kg, euthanized for reasons unrelated to this study. Each hemi-pelvis was radiographed, and TKR templates were superimposed on the radiographs to determine implant size. Hemi-pelvises were stored at -40°C and taken out to thaw at room temperature 24 hours in advance of testing. For specimen preparation, tissue above the hip joint was removed. Using holes drilled through the ischial tuberosity and sacroiliac joint of the ilium, a custom made bar of angle iron was bolted to the specimen. The

collateral ligaments were exposed; however, the specimen was left intact with no muscles or ligaments severed.

#### 2.4.2 Simulated Motion Cycle

Each specimen was mounted to a modified OKR by attaching the angle iron to the crosshead of an Instron testing machine (Figure 2.4). The Instron travelled at a rate of 50 cm/min to provide controlled vertical motion to simulate flexion and extension. The paw was attached to a platform with a dog boot that tightened below the hock without impeding range of motion of the hock joint. Sliders were adjusted to align the tibial crest directly over the paw at full extension. The modified OKR was used to simulate flexion by holding the paw rigid and displacing the angle iron at the proximal attachment of the specimen. The angle iron was free to rotate in the craniocaudal plane, simulating angular spinal movement. The specimen was also free to translate in the mediolateral and craniocaudal planes through the use of sliders, allowing the full six degrees of freedom of the stifle. Each specimen was cycled from full extension to full flexion (140°-90°) for five cycles while data was collected. Because the specimen started from a static position, the first cycle was not used in data analysis.

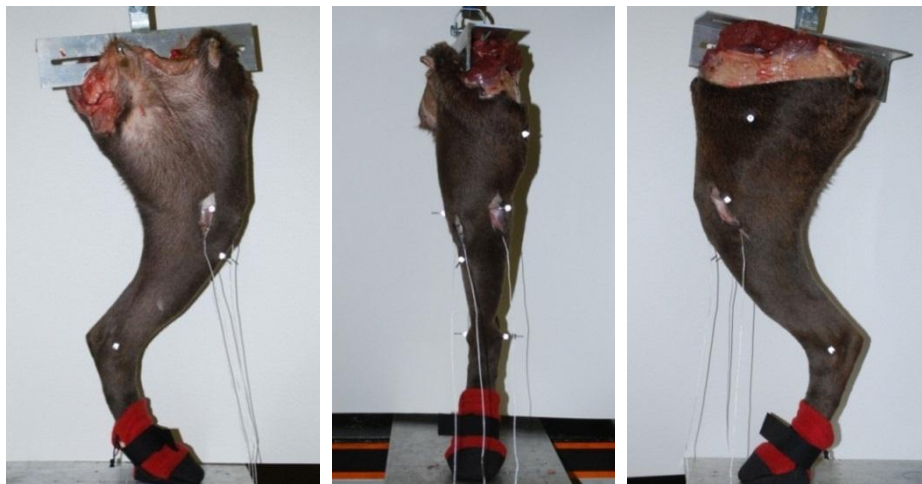


Figure 2.4: A canine specimen mounted on the modified OKR with the paw attached rigidly to a platform and the angle iron bolted through the ischial tuberosity and sacroiliac joint of the ilium. Reflective markers are visible as white dots. Displacement sensors are attached to the collateral ligaments.

### 2.4.3 Motion Tracking

After the specimen was mounted to the rig, Kirschner wire (1.6 mm diameter) was drilled into the bone at six anatomical locations (Figure 2.5), and reflective markers were attached to the end of each wire at the skin. Prior to testing, the stifle and hock joints underwent full range of motion to ensure no impingement from the wires. During the motion cycle, three-dimensional marker positions were collected with a set of five infrared cameras (Vicon T-series) at 200 Hz with Vicon Motus software.

Using the raw marker location data, the angular and translational motions of the stifle joint were calculated in Matlab with the joint coordinate system technique described by Fu et al.<sup>36</sup> Rotations about the three anatomical axes were calculated and reported as motion of the tibia relative to the femur. Translations were calculated from the tibial crest to the midpoint of the femoral epicondyles along the long femoral axis. Except for flexion/extension, kinematics were calculated in reference to the initial position at full extension with an angle of 0° or a translation of 0 mm indicating the joint was in the same orientation as the initial frame.

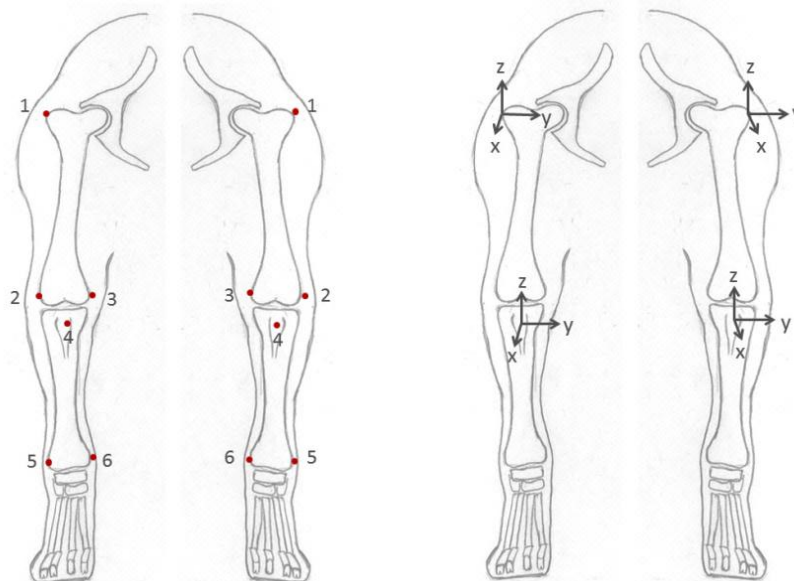


Figure 2.5: Canine hind limbs with marker locations shown in red and the constructed Joint Coordinate Systems located on the greater trochanter and tibial crest. Markers locations: 1-greater trochanter, 2-lateral epicondyle, 3-medial epicondyle, 4-tibial crest, 5-lateral malleolus, 6-medial malleolus. Joint coordinate system axes: x +cranial; y +lateral left leg/+medial right leg; z +proximal.

#### 2.4.4 Collateral Ligament Strain Measurement

Displacement sensors (MicroStrain, M-DVRT-3) are comprised of a main body and freely moving core and detect relative position by measuring the coils' differential reluctance using a sine wave excitation and synchronous demodulator (Figure 2.6).<sup>37-39</sup> Sensors were connected directly to a signal conditioner (MicroStrain, DEMOD-DVRT) calibrated at the factory with the sensors. A Vernier LabPro Data Logger and computer with software (Logger Pro 3.6.0) were used to collect the conditioned output voltage from the displacement sensors.

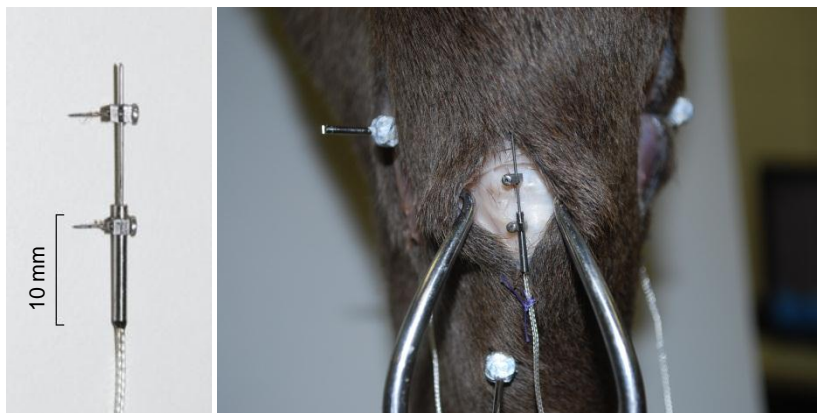


Figure 2.6: MicroStrain 3 mm displacement sensor (M-DVRT-3) with barbs (left) and attached to the patellar tendon (right).

The displacement sensors were attached to the lateral collateral ligament (LCL) and medial collateral ligament (MCL) using barbs on the sensor at locations marked with a fine tip marker to allow reattachment if removed. The long axis of each sensor was aligned with the long axis of the ligament with the specimen at full extension. The sensor wire was loosely sutured to the overlying tissue to prevent sensor displacement. For strain calculations, the original distance between the sensor barbs with the leg at full extension was measured with calipers ( $\pm 0.01$  mm). The sensors were left on the ligaments for the duration of the experiment. Extreme care was taken not to disturb sensor attachments during TKR; however, if sensors were inadvertently removed, they were replaced on the previously marked locations, and the distance between the barbs was re-measured. Displacement data was

collected at 200 Hz. Displacement for each sensor was calculated from output voltages using the factory calibration polynomial fit equations. Strain was calculated as the ratio of sensor displacement to original length between the barbs. Strain data was coordinated with the kinematic data using a custom Matlab program that determined the length of a motion cycle from the flexion/extension kinematic data and the point at which displacement values deviated from the baseline as a starting point.

#### 2.4.5 TKR Components

In order to determine the effects of tibial plateau angle and spacer thickness on the kinematics of the stifle and strain to the surrounding ligaments, tibial baseplates simulating three plateau angles were manufactured by BioMedtrix. Three tibial plateau angles (8, 4, 0°) and three tibial spacer thicknesses (5, 7, 9 mm) were investigated. Tibial baseplates were designed to be implanted on a 10° tibial cut performed by an extramedullary tibial alignment guide (ETAG). The tibial implant was comprised of two components: a set of three tibial baseplates that determined tibial plateau angle and three interchangeable spacers of varying thicknesses that snap-fit into the baseplates (Figure 2.7). The custom tibial baseplates were manufactured with three identical screw holes that allowed them to be screwed into the tibial osteotomy without altering the position of the baseplates between components. Femoral implant components and tibial spacers used during the procedure were stock components.

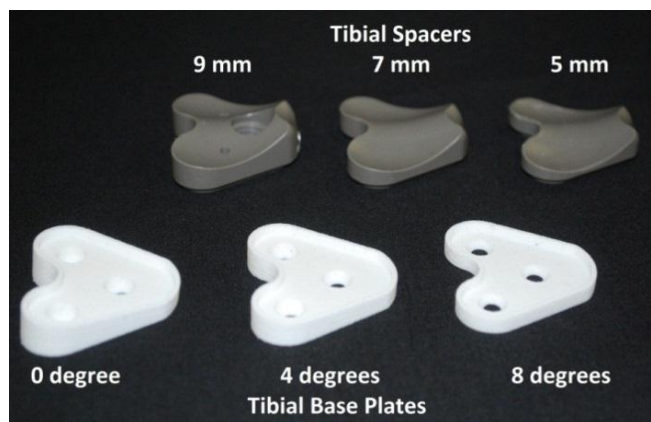


Figure 2.7: Stock tibial spacers from 5-9 mm commercially available from BioMedtrix (top) and custom tibial baseplates simulating 8, 4, and 0 degree tibial osteotomies.

#### 2.4.6 Experimental Procedure

During the first set of experiments, a baseline of the normal stifle was established for each specimen by mounting it to the OKR. Markers and sensors were placed at the previously listed anatomical locations by the same surgeon for each procedure, and the specimen was run from full extension to flexion for five cycles. While mounted on the rig, the surgeon opened the joint capsule and completely severed the CrCL. The specimen was again run through five cycles while collecting data, and then the reflective markers were removed while the displacement sensors and k-wires were left in place.

The specimen was then transported to the UGA veterinary school for a TKR procedure described by Liska and Doyle.<sup>6</sup> The same surgeon performed the TKR procedure for all test cases. An incision was made over the joint, and the patellar tendon was moved to the lateral side for access to the joint capsule. The menisci and cruciate ligaments were excised, taking care not to damage the collateral ligaments. The ETAG was drilled into place at the proximal and distal tibia with intramedullary pins, and a tibial osteotomy was performed at 10°. The ETAG was then removed, and a trial tibial implant component was inserted to check the fit with the joint. Holes were drilled to mark the locations of the tibial baseplate screws. The tibial component was removed, and the femoral alignment guide was drilled into place at the distal femur, taking care to avoid k-wire locations. A femoral osteotomy was performed, and the alignment guide removed so the femoral component could be press fit into place. The 8° tibial baseplate was then screwed into place, and the 5 mm custom tibial spacer was snap-fit onto the baseplate. With the joint reduced, the patellar tendon was replaced in its natural position, and the fit of the implant was tested by extending and flexing the joint. The surgeon then closed the joint capsule and overlying tissue with bowtie sutures to facilitate re-opening of the joint to switch out implant components.

The specimen was transported back to the testing lab and remounted on the rig with its position at full extension replicated. The reflective tracking markers were replaced, and the specimen was run for

five cycles while marker location and ligament displacement were recorded. The specimen remained on the rig with markers and sensors in place while the custom tibial spacer implants were changed out in order of increasing thickness. To interchange the spacers, the bowtie sutures were released, the joint flexed and the tibia cranially luxated for access to the implant (Figure 2.8). The previous spacer was snapped out of place and replaced with the next largest spacer with the joint flexed. The leg was reduced with pressure applied on the spacer to move the femoral component into the spacer tracks.

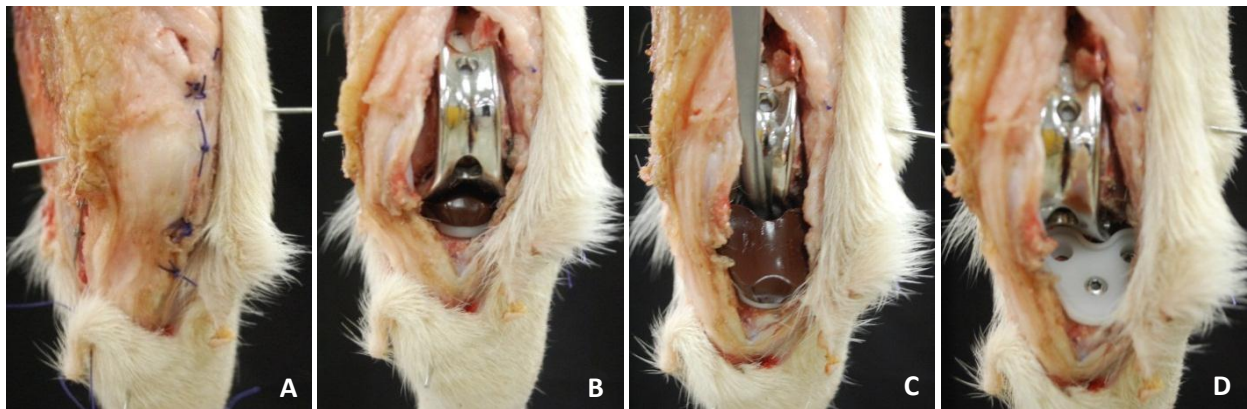


Figure 2.8: Cranial views of (A) the stifle joint closed with sutures; (B) the stifle joint exposed; (C) the proximal tibia cranially luxated for access to the tibial components; (D) the tibial spacer removed exposing the tibial baseplate.

Once all three spacer thicknesses were tested at  $8^\circ$ , the tibial baseplate was removed, and the  $4^\circ$  baseplate implanted. With the  $4^\circ$  baseplate, the 5 mm and 7 mm spacers were tested in order of increasing thickness. The  $4^\circ$  baseplate was then replaced with the  $0^\circ$  baseplate and tested with only the 5 mm spacer. Baseplates with decreasing angles were tested with only the thinner spacers to avoid over stuffing the joint and damaging the surrounding ligaments during testing. Each specimen was run through five motion cycles with each set of implants. A final radiograph was taken to determine any differences between target and actual tibial plateau angle.

## 2.4.7 Statistical Analysis

Mean peak values were calculated for each trial within specimen and used for a paired t-test. The questions of interest were: was there significant variability within specimen in kinematics or strain between TKR trials implanted (1) with varying tibial plateau angles and (2) with varying tibial spacer thicknesses. All statistical analyses were calculated in Minitab (release 13 for Windows). Comparisons with a paired t-test were performed to determine if there were significant differences in kinematic and strain data due to plateau angle and spacer thickness. A significance level of  $p < 0.05$  was used for all analyses.

## 2.5 Results

### 2.5.1 Normal versus CrCL Deficient Stifle

A summary of all kinematic and strain data is shown in Table 2.3. CrCL transection caused a decrease in lateral translation by an average of  $1.3 \pm 1.0$  mm. CrCL transection did not significantly alter any other kinematics or strain to the collateral ligaments.

Table 2.3: Mean Peak Kinematics and Ligament Strain of the Normal and CrCL Transected Stifles. Kinematics are reported as motion of the tibia relative to the femur during flexion.

\* indicates significant difference ( $p < 0.05$ ) within a column using a paired t-test.

|                    |          | Rotations (degrees)       |                         | Translations (mm)    |                      |                       | Strain (%) |      |
|--------------------|----------|---------------------------|-------------------------|----------------------|----------------------|-----------------------|------------|------|
|                    |          | +Adduction/<br>-Abduction | +External/<br>-Internal | +Cranial/<br>-Caudal | +Lateral/<br>-Medial | +Proximal/<br>-Distal | MCL        | LCL  |
| Normal             | Peak     | 4.3                       | -8.9                    | -20.0                | 6.2*                 | -14.0                 | 0.11       | 5.72 |
|                    | $\pm$ SD | 2.8                       | 5.5                     | 5.5                  | 5.9                  | 4.3                   | 0.03       | 1.08 |
| CrCL<br>Transected | Peak     | 1.2                       | -7.8                    | -20.4                | 4.9*                 | -15.5                 | 0.25       | 7.02 |
|                    | $\pm$ SD | 5.2                       | 4.5                     | 5.5                  | 4.3                  | 4.0                   | 0.23       | 4.90 |

### 2.5.2 Tibial Plateau Angle

The postoperative plateau angle among specimens was  $10.2 \pm 1.8^\circ$  (Figure 2.9). A summary of all kinematic and strain data is shown in Table 2.4 and Figures 2.10-2.16. All baseplates paired with the 5 mm spacer caused a significant decrease in distal translation by an average of 5.9 mm that did not vary

significantly between baseplates. All baseplates also caused a significant increase in caudal tibial thrust by an average of 3.2 mm. Compared to the normal stifle, TKR with an 8 degree baseplate also caused a decrease in both internal rotation by 5° and lateral translation by 4.1 mm. TKR with the 8 degree baseplate did not significantly alter adduction. Both the 4 degree and 0 degree implants caused a significant reversal from adduction to  $2.8 \pm 4.6^\circ$  and  $4.0 \pm 3.7^\circ$  abduction, from internal rotation to  $5.1 \pm 6.9^\circ$  and  $6.5 \pm 8.0^\circ$  external rotation, and from lateral translation to  $7.3 \pm 3.1$  mm and  $8.7 \pm 4.7$  mm medial translation respectively.

Compared to the normal stifle, the 8 degree and 4 degree baseplates significantly decreased LCL strain to  $0.49 \pm 0.53\%$  and  $0.21 \pm 0.09\%$  respectively. The 0 degree baseplate returned LCL strain to  $7.63 \pm 1.65\%$ , which was not significantly different from normal. There were no significant differences in strain to the MCL between the normal stifle and any of the treatments.



Figure 2.9: Postoperative radiograph with a 10° tibial plateau angle showing implant components and k-wire pins.

Table 2.4: Mean Peak Kinematics and Ligament Strain among Tibial Plateau Angles. Kinematics are reported as motion of the tibia relative to the femur during flexion. Rotations/translations within a column with different superscripts are significantly different ( $p < 0.05$ ) using a paired t-test.

|                    |      | Rotations (degrees)       |                         | Translations (mm)    |                      |                       | Strain (%) |                   |
|--------------------|------|---------------------------|-------------------------|----------------------|----------------------|-----------------------|------------|-------------------|
|                    |      | +Adduction/<br>-Abduction | +External/<br>-Internal | +Cranial/<br>-Caudal | +Lateral/<br>-Medial | +Proximal/<br>-Distal | MCL        | LCL               |
| Normal             | Peak | 4.3 <sup>a</sup>          | -8.9 <sup>a</sup>       | -20.0 <sup>a</sup>   | 6.2 <sup>a</sup>     | -14.0 <sup>a</sup>    | 0.11       | 5.72 <sup>a</sup> |
|                    | ±SD  | 2.8                       | 5.5                     | 5.5                  | 5.9                  | 4.3                   | 0.03       | 1.08              |
| CrCL<br>Transected | Peak | 1.2 <sup>ab</sup>         | -7.8 <sup>ab</sup>      | -20.4 <sup>ab</sup>  | 4.9 <sup>b</sup>     | -15.5 <sup>a</sup>    | 0.25       | 7.02 <sup>a</sup> |
|                    | ±SD  | 5.2                       | 4.5                     | 5.5                  | 4.3                  | 4.0                   | 0.23       | 4.90              |
| 8deg 5mm           | Peak | 4.3 <sup>a</sup>          | -3.9 <sup>b</sup>       | -22.0 <sup>bc</sup>  | 2.1 <sup>b</sup>     | -8.4 <sup>b</sup>     | 0.02       | 0.49 <sup>b</sup> |
|                    | ±SD  | 2.5                       | 4.3                     | 5.3                  | 7.3                  | 3.6                   | 0.03       | 0.53              |
| 4deg 5mm           | Peak | -2.8 <sup>bc</sup>        | 5.1 <sup>c</sup>        | -24.4 <sup>b</sup>   | -7.3 <sup>c</sup>    | -8.0 <sup>b</sup>     | 0.67       | 0.21 <sup>b</sup> |
|                    | ±SD  | 4.6                       | 6.9                     | 3.6                  | 3.1                  | 4.3                   | 0.99       | 0.09              |
| 0deg 5mm           | Peak | -4.0 <sup>c</sup>         | 6.5 <sup>c</sup>        | -23.3 <sup>c</sup>   | -8.7 <sup>c</sup>    | -7.9 <sup>b</sup>     | 0.50       | 7.63 <sup>a</sup> |
|                    | ±SD  | 3.7                       | 8.0                     | 4.0                  | 4.7                  | 3.9                   | 0.40       | 1.65              |

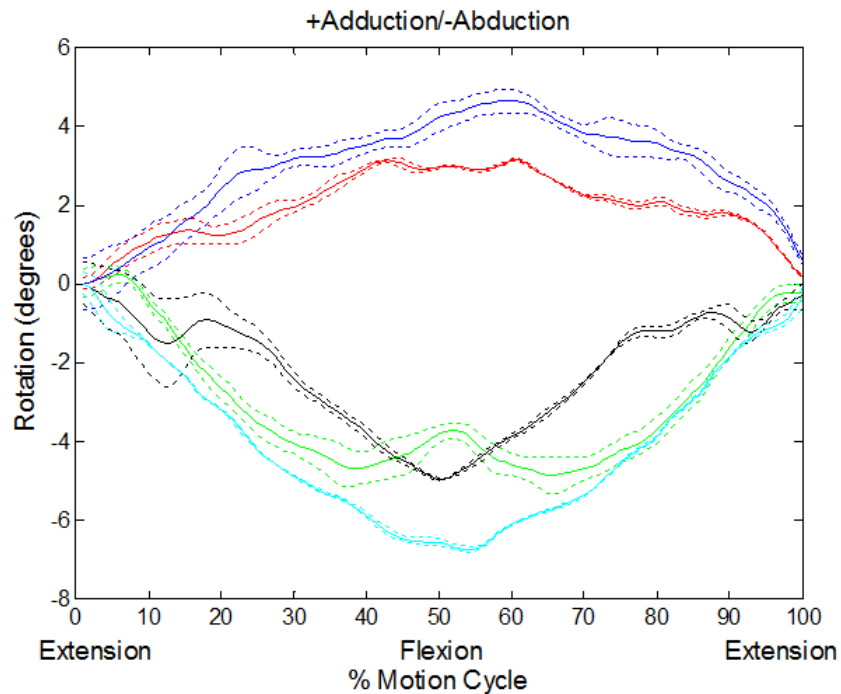


Figure 2.10: Mean adduction among plateau angles for a specimen with standard deviations. **Red**- Normal, **Green**- CrCL transected, **Blue**- 8deg 5mm, **Black**- 4deg 5mm, **Cyan**- 0deg 5mm

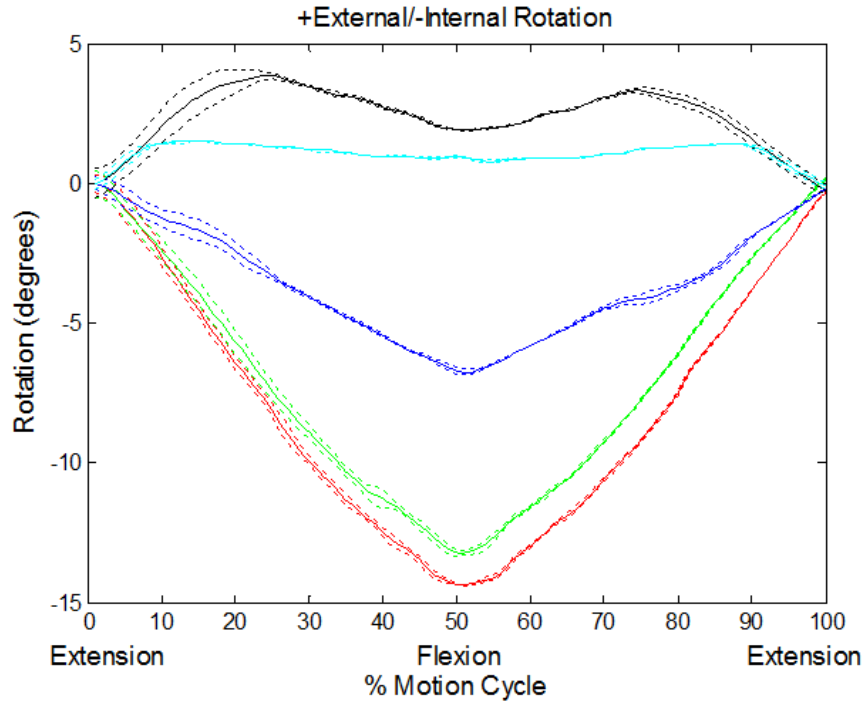


Figure 2.11: Mean external rotation among plateau angles for a specimen with standard deviations. **Red**- Normal, **Green**- CrCL transected, **Blue**- 8deg 5mm, **Black**- 4deg 5mm, **Cyan**- 0deg 5mm

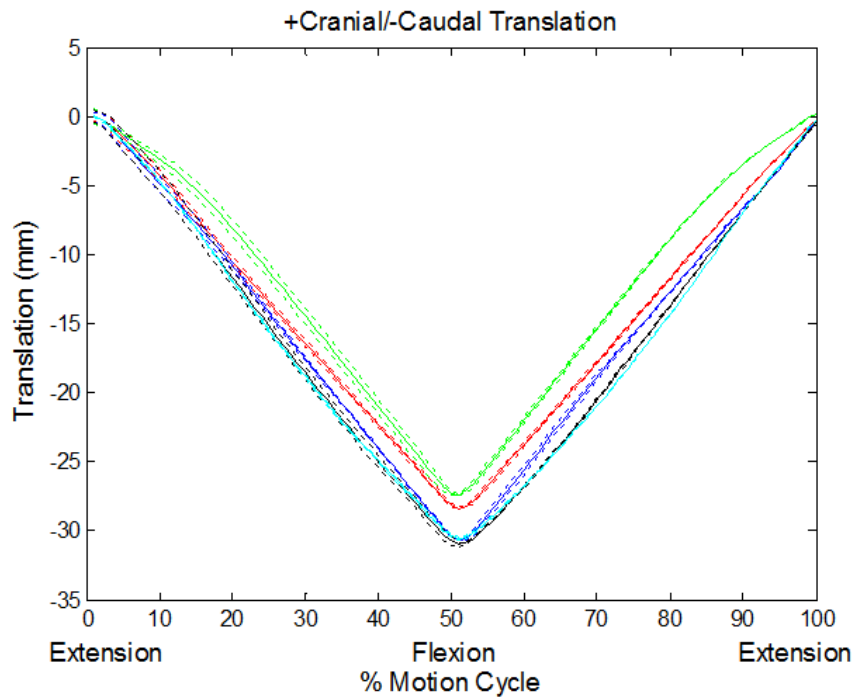


Figure 2.12: Mean cranial translation among plateau angles for a specimen with standard deviations. **Red**- Normal, **Green**- CrCL transected, **Blue**- 8deg 5mm, **Black**- 4deg 5mm, **Cyan**- 0deg 5mm

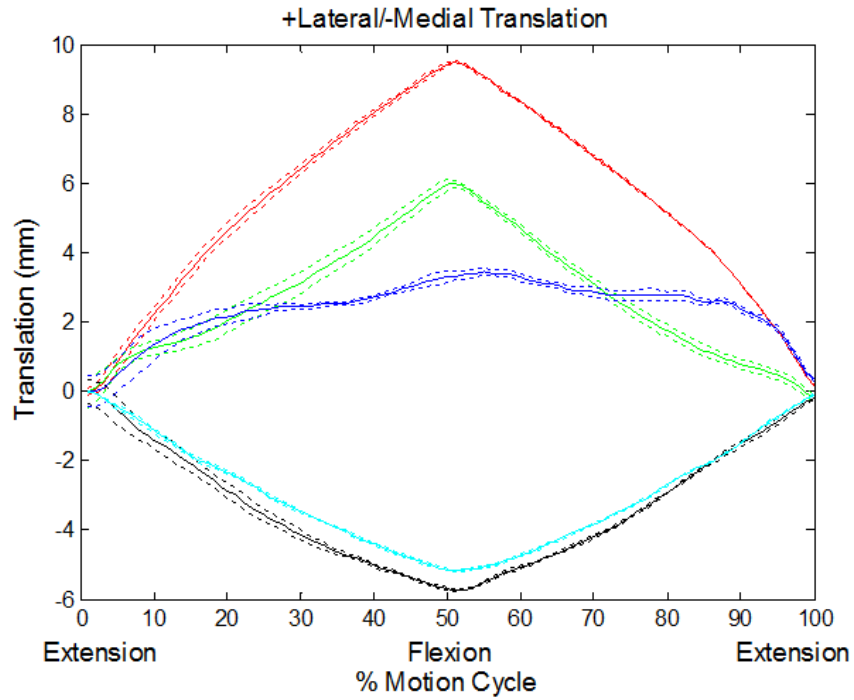


Figure 2.13: Mean lateral translation among plateau angles for a specimen with standard deviations. **Red**- Normal, **Green**- CrCL transected, **Blue**- 8deg 5mm, **Black**- 4deg 5mm, **Cyan**- 0deg 5mm

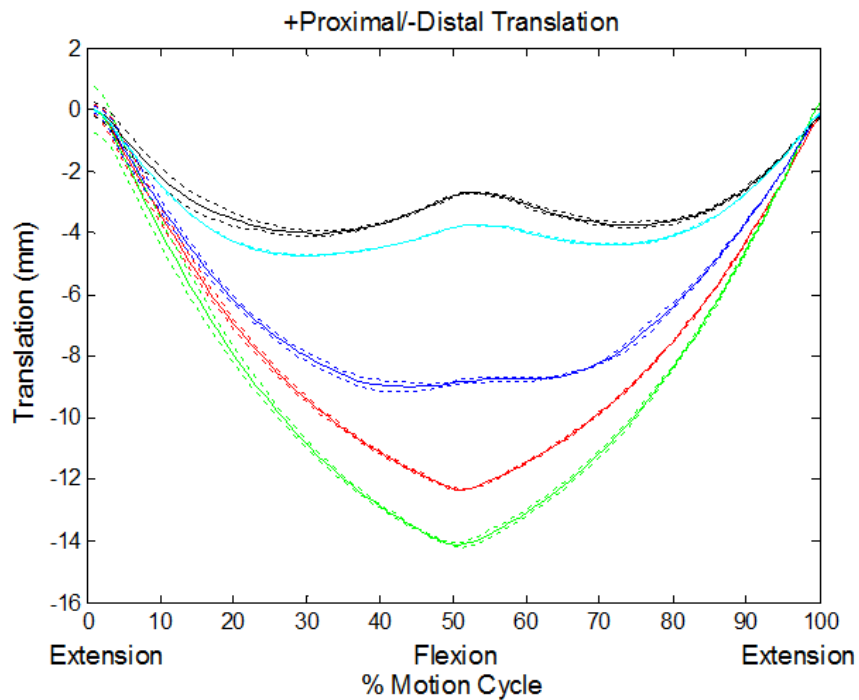


Figure 2.14: Mean proximal translation among plateau angles for a specimen with standard deviations. **Red**- Normal, **Green**- CrCL transected, **Blue**- 8deg 5mm, **Black**- 4deg 5mm, **Cyan**- 0deg 5mm

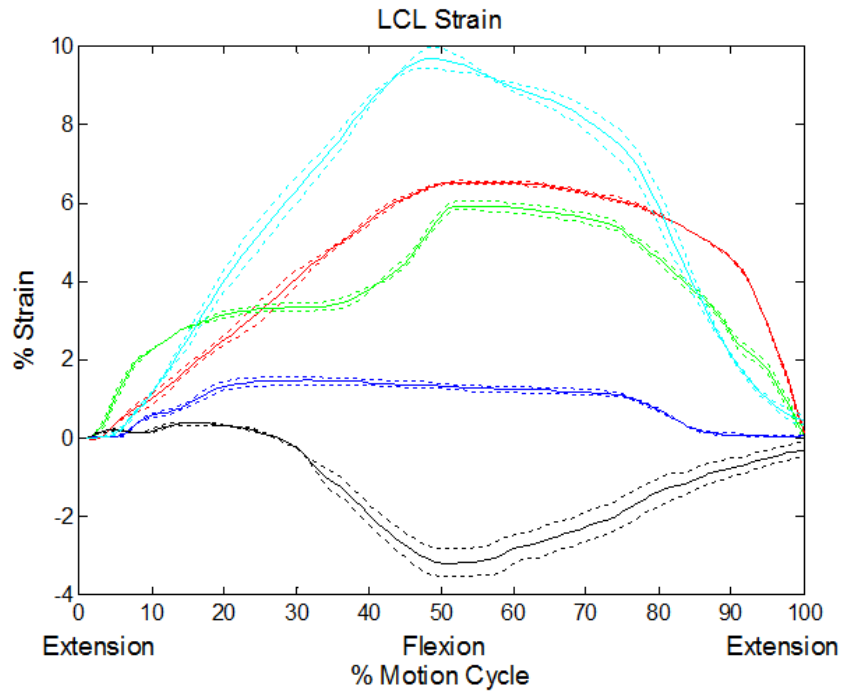


Figure 2.15: Mean lateral collateral ligament strain among plateau angles for a specimen with standard deviations.

Red- Normal, Green- CrCL transected, Blue- 8deg 5mm, Black- 4deg 5mm, Cyan- 0deg 5mm

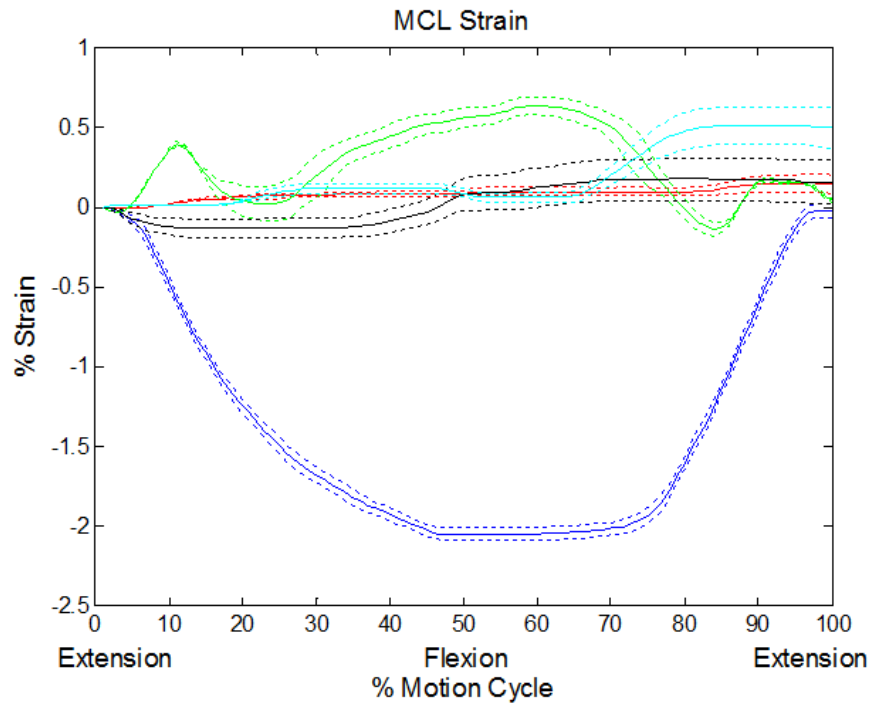


Figure 2.16: Mean medial collateral ligament strain among plateau angles for a specimen with standard deviations.

Red- Normal, Green- CrCL transected, Blue- 8deg 5mm, Black- 4deg 5mm, Cyan- 0deg 5mm

### 2.5.3 Tibial Spacer Thickness

A summary of all kinematic and strain data is shown in Table 2.5 and Figures 2.17-2.23. As previously reported, the 8 degree 5 mm spacer caused a significant decrease in internal rotation, lateral translation, and proximal translation as well as a significant increase in caudal translation. The 7 mm and 9 mm spacers caused a significant decrease in adduction to  $1.6 \pm 5.8^\circ$  and  $1.6 \pm 1.6^\circ$  respectively. The 7 mm and 9 mm spacers caused a significant reversal to external rotations of  $1.9 \pm 1.0^\circ$  and  $0.5 \pm 4.4^\circ$  respectively. Both the 7 mm and 9 mm spacers caused significant excess caudal tibial translation by an average of 4.7 mm that did vary significantly between spacers. The 7 mm spacer caused a reversal from lateral translation to  $4.7 \pm 4.9$  mm medial translation, while the 9 mm spacer caused a significant decrease in lateral translation by 5.1 mm. TKR with all three spacers caused a decrease in proximal translation by 5.3 mm that did not vary significantly between implants.

Compared to the normal stifle, TKR with all three spacer thicknesses significantly decreased LCL strain from 5.72% to an average of 0.61% which did not vary significantly between spacers. There were no significant differences in strain to the MCL between the normal and CrCL transected stifle and any of the spacer thicknesses.

Table 2.5: Mean Peak Kinematics and Ligament Strain Among Tibial Spacer Thickness. Kinematics are reported as motion of the tibia relative to the femur during flexion. Rotations/translations within a column with different superscripts are significantly different ( $p < 0.05$ ) using a paired t-test.

|                    |      | Rotations (degrees)       |                         | Translations (mm)    |                      |                       | Strain (%) |                   |
|--------------------|------|---------------------------|-------------------------|----------------------|----------------------|-----------------------|------------|-------------------|
|                    |      | +Adduction/<br>-Abduction | +External/<br>-Internal | +Cranial/<br>-Caudal | +Lateral/<br>-Medial | +Proximal/<br>-Distal | MCL        | LCL               |
| Normal             | Peak | 4.3 <sup>a</sup>          | -8.9 <sup>a</sup>       | -20.0 <sup>a</sup>   | 6.2 <sup>a</sup>     | -14.0 <sup>a</sup>    | 0.11       | 5.72 <sup>a</sup> |
|                    | ±SD  | 2.8                       | 5.5                     | 5.5                  | 5.9                  | 4.3                   | 0.03       | 1.08              |
| CrCL<br>Transected | Peak | 1.2 <sup>ab</sup>         | -7.8 <sup>ab</sup>      | -20.4 <sup>ab</sup>  | 4.9 <sup>b</sup>     | -15.5 <sup>a</sup>    | 0.25       | 7.02 <sup>a</sup> |
|                    | ±SD  | 5.2                       | 4.5                     | 5.5                  | 4.3                  | 4.0                   | 0.23       | 4.90              |
| 8deg 5mm           | Peak | 4.3 <sup>ab</sup>         | -3.9 <sup>b</sup>       | -22.0 <sup>b</sup>   | 2.1 <sup>bc</sup>    | -8.4 <sup>b</sup>     | 0.02       | 0.49 <sup>b</sup> |
|                    | ±SD  | 2.5                       | 4.3                     | 5.3                  | 7.3                  | 3.6                   | 0.03       | 0.53              |
| 8deg 7mm           | Peak | 1.6 <sup>b</sup>          | 1.9 <sup>c</sup>        | -24.4 <sup>b</sup>   | -4.7 <sup>c</sup>    | -7.5 <sup>b</sup>     | 0.07       | 0.09 <sup>b</sup> |
|                    | ±SD  | 5.8                       | 1.0                     | 4.4                  | 4.9                  | 5.3                   | 0.09       | 0.12              |
| 8deg 9mm           | Peak | 1.6 <sup>b</sup>          | 0.5 <sup>c</sup>        | -24.9 <sup>b</sup>   | 1.1 <sup>bc</sup>    | -8.9 <sup>b</sup>     | 0.62       | 1.25 <sup>b</sup> |
|                    | ±SD  | 1.6                       | 4.4                     | 5.5                  | 3.1                  | 6.8                   | 0.88       | 1.23              |

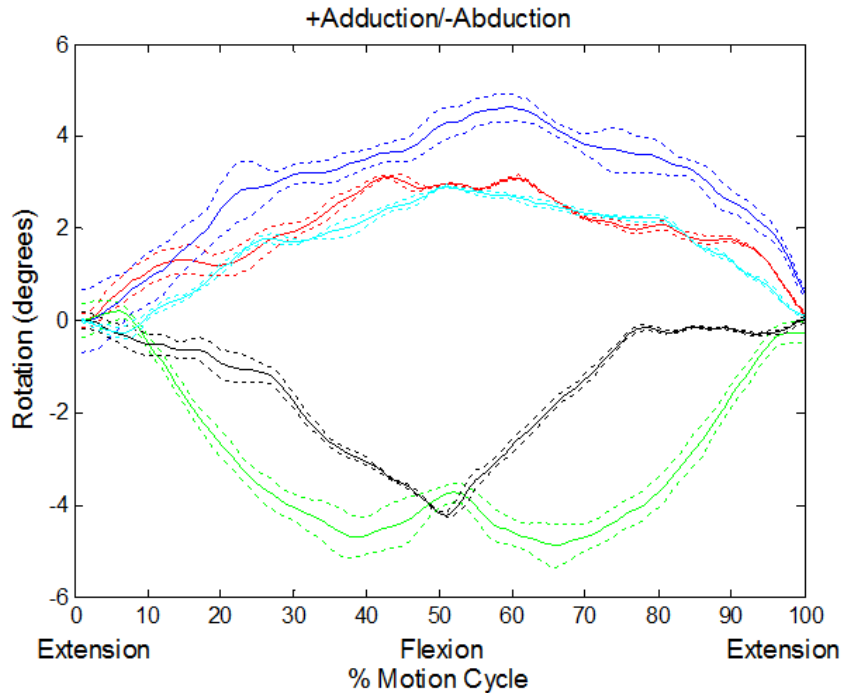


Figure 2.17: Mean adduction among tibial spacer thickness for a specimen with standard deviations. Red- Normal, Green- CrCL transected, Blue- 8deg 5mm, Black- 8deg 7mm, Cyan- 8deg 9mm

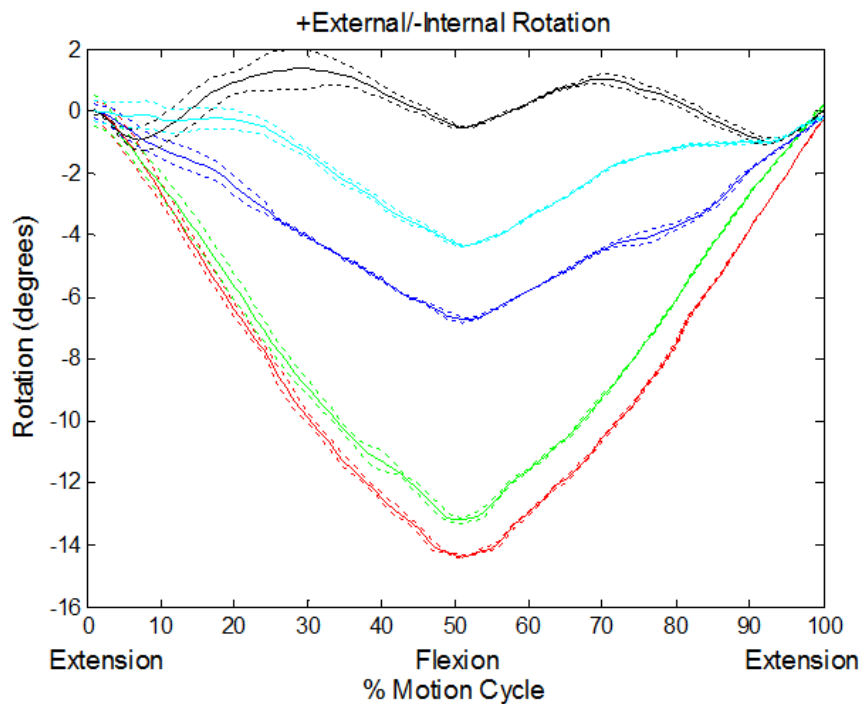


Figure 2.18: Mean external rotation among tibial spacer thickness for a specimen with standard deviations.

Red- Normal, Green- CrCL transected, Blue- 8deg 5mm, Black- 8deg 7mm, Cyan- 8deg 9mm

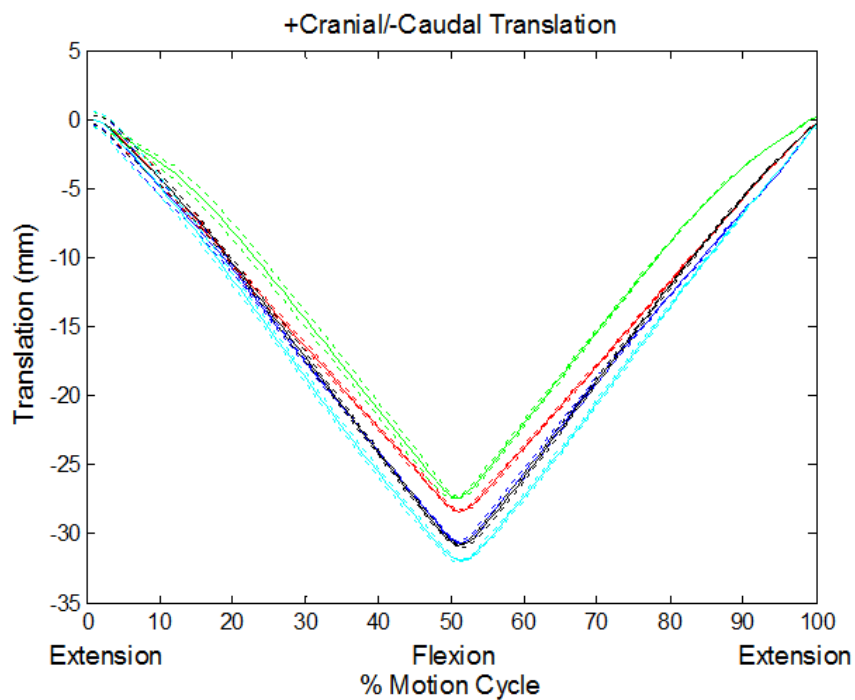


Figure 2.19: Mean cranial translation among tibial spacer thickness for a specimen with standard deviations.

Red- Normal, Green- CrCL transected, Blue- 8deg 5mm, Black- 8deg 7mm, Cyan- 8deg 9mm

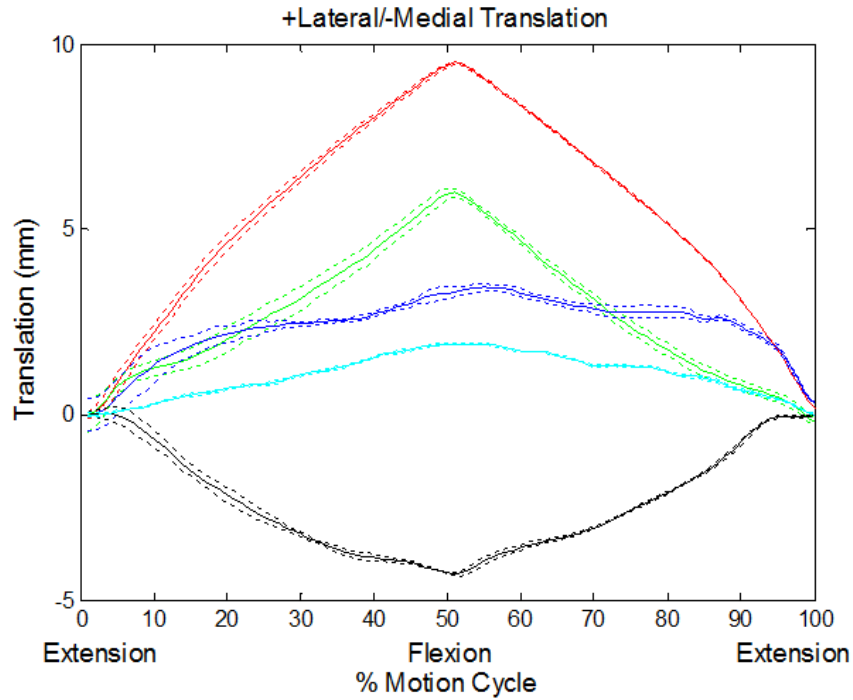


Figure 2.20: Mean lateral translation among tibial spacer thickness for a specimen with standard deviations.

Red- Normal, Green- CrCL transected, Blue- 8deg 5mm, Black- 8deg 7mm, Cyan- 8deg 9mm

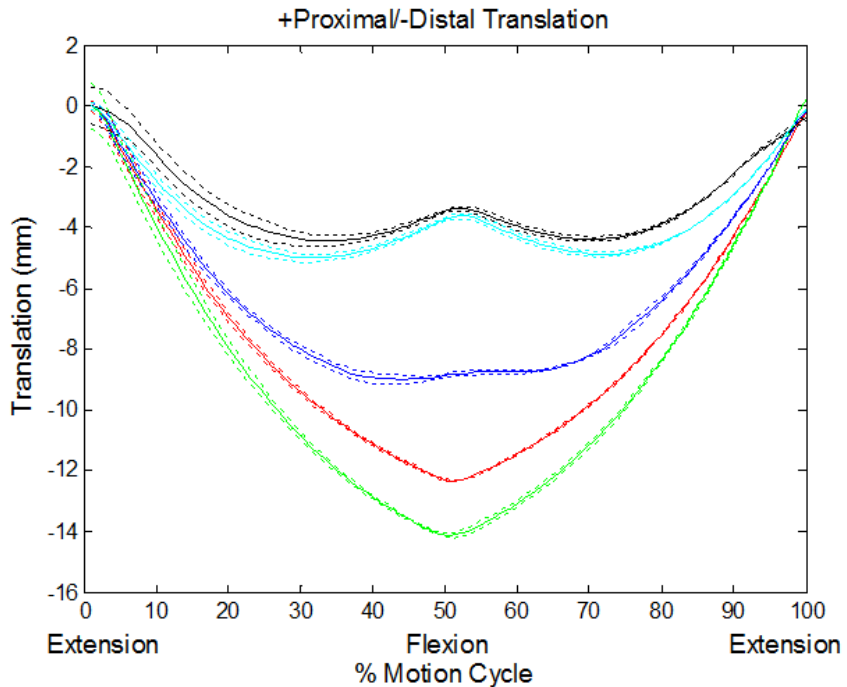


Figure 2.21: Mean proximal translation among tibial spacer thickness for a specimen with standard deviations.

Red- Normal, Green- CrCL transected, Blue- 8deg 5mm, Black- 8deg 7mm, Cyan- 8deg 9mm

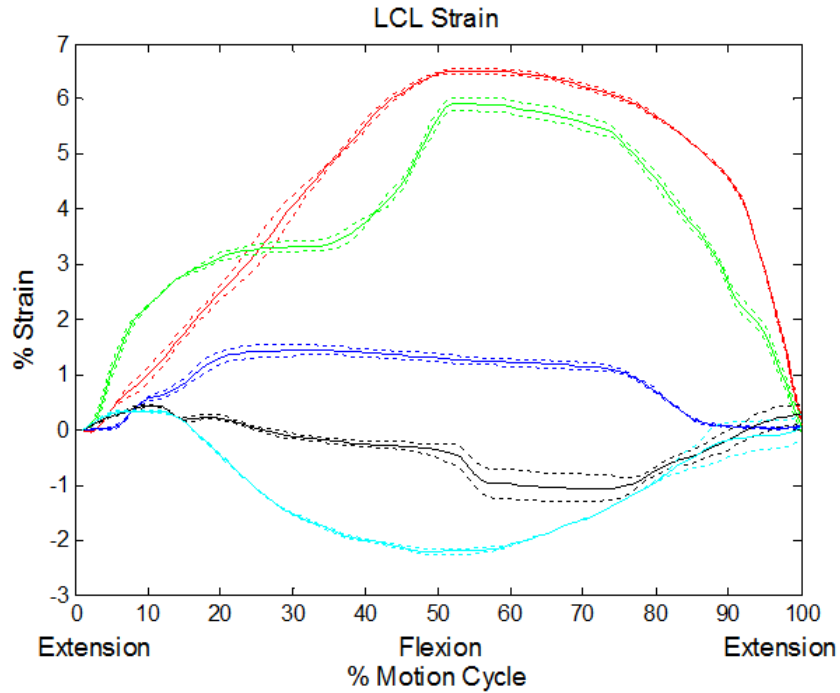


Figure 2.22: Mean lateral collateral ligament strain among tibial spacer thickness for a specimen with standard deviations.

**Red-** Normal, **Green-** CrCL transected, **Blue-** 8deg 5mm, **Black-** 8deg 7mm, **Cyan-** 8deg 9mm

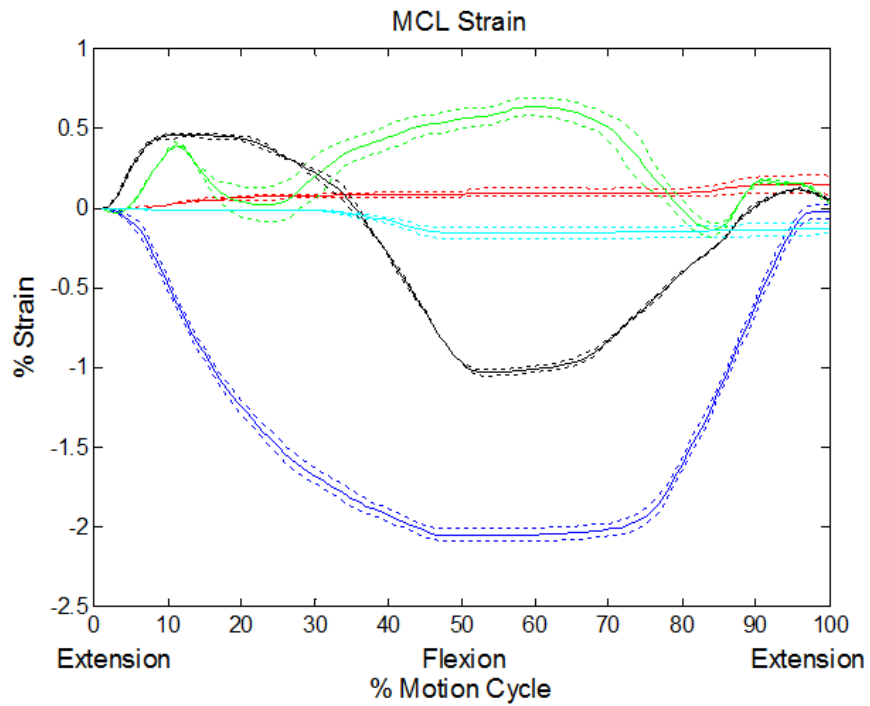


Figure 2.23: Mean medial collateral ligament strain among tibial spacer thickness for a specimen with standard deviations.

**Red-** Normal, **Green-** CrCL transected, **Blue-** 8deg 5mm, **Black-** 8deg 7mm, **Cyan-** 8deg 9mm

## 2.6 Discussion

Joint rotations of the normal stifle in this study were comparable to *in vivo* results published by Fu et al.,<sup>36</sup> which reported average stifle rotations of six canines during a walking gait from approximately 140° extension to 115° flexion. Stifle joints *in vivo* showed approximately 10° internal rotation of the tibia relative to the femur during flexion, similar to the 8.9° of internal rotation in this study. Stifle joints *in vivo* also showed 10° adduction compared to the 4.2° of adduction in this study.

No previous studies have been found quantitatively investigating the effects of total knee replacement on canine stifle kinematics either *in vitro* or *in vivo*; however, multiple studies have looked at the effects of CrCL transection and other reconstruction techniques. *In vitro* canine studies that simulated the pull of the gastrocnemius and quadriceps muscles reported significant increases in cranial tibial translation and internal rotation after transection of the CrCL which were not seen in this study.<sup>20,25</sup> However, Korvick et al.<sup>40</sup> reported from an *in vivo* study of five canines that excess cranial tibial thrust in the CrCL deficient stifle only occurs during the stance phase with the joint returning to normal craniocaudal alignment during the non-weight bearing swing phase. It has also been shown that quadriceps pull generates a force in the CrCL at certain flexion angles indicating that the quadriceps is a contributor cranial tibial thrust.<sup>41-43</sup> Since the present study used passive flexion of the joint without simulating weight bearing or active quadriceps forces, it is not surprising that cranial tibial thrust was not observed after CrCL transection.

Kinematics after CrCL transection in this study were similar to results from the *in vitro* canine study by Chailleux et al.,<sup>34</sup> which pulled on the quadriceps tendon but did not simulate weight bearing. After CrCL transection, no significant changes were seen in cranial tibial thrust, adduction, or internal rotation. These results were attributed to the fact that only the non-weight bearing phase of gait was simulated. It was concluded that quadriceps force is not the main proponent of cranial tibial translation and that a weight bearing simulation coupled with quadriceps pull would have likely caused significant cranial tibial

thrust. This conclusion is further supported by a study by Reif et al.<sup>26</sup> in which an axial load was applied to canine cadaver stifles without simulating muscle forces. Significant cranial tibial translation was observed after CrCL transection, indicating that weight bearing without simulation of a quadriceps force places a significant load on the CrCL. Results from these previous *in vitro* studies support the results from the present study in which no significant changes in joint rotations were seen after CrCL transection in the canine stifle flexed passively.

All implant combinations caused a significant decrease in distal tibial translation that was not significant between implants as well as an increase in caudal tibial thrust. The decrease in distal translation indicates that the TKR components did not fill as much of the joint space as was removed with the osteotomies. Even though the 9 mm spacer showed the largest distal translation, an increase in spacer thickness was not enough to increase distal translation significantly. As expected, there was an increase in caudal tibial translation after TKR with all implants. This may be attributed to the significant decrease in tibial plateau angle as compared to the natural 24° plateau seen in the canine stifle. With the caudal cruciate ligament no longer intact, the shallower slope prevents excess cranial tibial thrust but causes excess caudal tibial thrust. Therefore, even steeper tibial plateaus than 8 degrees should be investigated to determine if the stifle kinematics are restored more closely to normal.

The initial 8 degree 5 mm implant restored adduction to normal. While this implant also significantly decreased internal rotation by 5°, it was the only baseplate that maintained the internal rotation of the stifle instead of reversing to external rotation. Tibial plateau angle significantly affected joint kinematics; decreasing the plateau angle to 4 and 0 degrees caused a reversal in kinematics to 2.8° and 4.0° abduction, 5.1° and 6.5° external rotation, and 7.3 mm and 8.7 mm medial translation respectively. These results indicate that shallower plateau angles incrementally cause a reversal from normal kinematics in adduction, internal rotation, and lateral translation. Tibial spacer thickness significantly

affected joint kinematics as well. Increasing spacer thickness to 7 mm and 9 mm caused significant decreases in adduction, a reversal to external rotation, and a decrease in lateral translation.

Strain to the MCL was minimal in the normal stifle and was not significantly different from normal after TKR. The 8 degree and 4 degree implants significantly decreased LCL strain, while 0 degree implant returned LCL strain to normal. These results indicate that strain to the LCL is minimal with steeper plateau angles, and the LCL may benefit from steeper tibial osteotomies. All three spacer thicknesses showed a significant decrease in LCL strain with an average of 0.61% that was not affected by increasing spacer thickness. The decreased strain on the collaterals may be attributed to the decreased distal tibial translations seen after TKR as the joint is more compact, causing less strain on the ligaments. Results from this study indicate that strain to the collateral ligaments is not negatively affected by TKR.

## 2.7 Conclusion

The study herein described the three-dimensional kinematics of the canine stifle before and after CrCL transection followed by total knee replacement with varying tibial plateau angles and spacer thicknesses. Transection of the CrCL did not significantly alter kinematics in this study except lateral translation, but is expected to cause excess cranial tibial translation during weight bearing conditions. Results from this study suggest that both tibial plateau angle and spacer thickness affect the kinematics of the canine stifle. Decreasing the plateau angle caused a reversal in adduction, internal rotation, and lateral translation. Increasing tibial spacer thickness caused a decrease in adduction, a reversal to external rotation, and a decrease in lateral translation. Abnormal knee kinematics in humans have been shown to cause a change in the contact mechanics of the implant, leading to premature implant wear and loosening as well as excess strain on the surrounding ligaments.<sup>44-46</sup> Abnormal kinematics due to these tibial implant variables may be a contributor to the implant complications and failures that have been observed clinically. Surgeons should take care not to cut the tibial plateau too shallow during

surgery or over stuff the joint with larger tibial spacers, as postoperative stifle kinematics and success rates are likely to be negatively affected.

Further studies should investigate plateau angles steeper than 8 degrees to determine if there is an angle where kinematics are more closely restored to normal. Future studies would also benefit from using a knee rig that includes a weight bearing force to more accurately simulate *in vivo* conditions that affect strain to the CrCL and joint kinematics. The results herein may serve as a foundation for the investigation of the optimal tibial plateau angle in canine total knee replacement and lead to increased success rates and quality of life for canines with stifle osteoarthritis.

## 2.8 References

1. Canapp Jr SO. The Canine Stifle. *Clin Tech Small Anim Pract* 2007;22:195-205.
2. Carpenter DH, Cooper RC. Mini Review of Canine Stifle Joint Anatomy. *Anat Histol Embryol* 2000;29:321-329.
3. De Rooster H, De Bruin T, Van Bree H. Morphologic and Functional Features of the Canine Cruciate Ligaments. *Vet Surg* 2006;35:769-780.
4. Wilke VL, Robinson DA, Evans RB, et al. Estimate of the annual economic impact of treatment of cranial cruciate ligament injury in dogs in the United States. *J Am Vet Med Assoc* 2005;227:1604-1607.
5. Witsberger TH, Villamil JA, Schultz LG, et al. Prevalence of and risk factors for hip dysplasia and cranial cruciate ligament deficiency in dogs. *J Am Vet Med Assoc* 2008;232:1818-1824.
6. Liska W, Doyle N. Canine total knee replacement: surgical technique and one-year outcome. *Vet Surg* 2009;38:568-582.
7. Preston C, Lidbetter D. Total Knee Replacement in Dogs, in Proceedings. ACVSc College Science Week 2009;36-39.
8. Tashman S, Anderst W, Kolowich P, et al. Kinematics of the ACL-deficient canine knee during gait: serial changes over two years. *J Orthop Res* 2004;22:931-941.
9. Gilbertson EM. Development of periarticular osteophytes in experimentally induced osteoarthritis in the dog. A study using microradiographic, microangiographic, and fluorescent bone-labelling techniques. *Ann Rheum Dis* 1975;34:12-25.
10. Andriacchi TP, Dyrby CO, Johnson TS. The use of functional analysis in evaluating knee kinematics. *Clin Orthop Relat Res* 2003;44-53.
11. Bergfeld JA, McAllister DR, Parker RD, et al. The effects of tibial rotation on posterior translation in knees in which the posterior cruciate ligament has been cut. *J Bone Joint Surg Am* 2001;83:1339-1343.
12. Baroni E, Matthias RR, Marcellin-Little DJ, et al. Comparison of radiographic assessments of the tibial plateau slope in dogs. *Am J Vet Res* 2003;64:586-589.
13. Aragon CL, Budsberg SC. Applications of evidence-based medicine: cranial cruciate ligament injury repair in the dog. *Vet Surg* 2005;34:93-98.
14. Cook JL, Luther JK, Beetem J, et al. Clinical comparison of a novel extracapsular stabilization procedure and tibial plateau leveling osteotomy for treatment of cranial cruciate ligament deficiency in dogs. *Vet Surg* 2010;39:315-323.
15. Dulisch ML. Suture reaction following extra-articular stifle stabilization in the dog. I. A retrospective study of 161 stifles. *J Am Anim Hosp Assoc* 1981;17:569-571.
16. Hoffmann DE, Martin RA, Shires PK, et al. Tibial tuberosity advancement in 65 canine stifles. *Vet Comp Orthop Traumatol* 2006;19:219-227.

17. Lafaver S, Miller NA, Stubbs WP, et al. Tibial tuberosity advancement for stabilization of the canine cranial cruciate ligament-deficient stifle joint: surgical technique, early results, and complications in 101 dogs. *Vet Surg* 2007;36:573-586.
18. Dupuis J, Gallina AM, Ratzlaff M, et al. Evaluation of fibular head transposition for repair of experimental cranial cruciate ligament injury in dogs. *Vet Surg* 1994;23:1-12.
19. Mullen HS, Matthiesen DT. Complications of transposition of the fibular head for stabilization of the cranial cruciate-deficient stifle in dogs: 80 cases (1982-1986). *J Am Vet Med Assoc* 1989;195:1267-1271.
20. Corr SA, Brown C. A comparison of outcomes following tibial plateau levelling osteotomy and cranial tibial wedge osteotomy procedures. *Vet Comp Orthop Traumatol* 2007;20:312-319.
21. Kim SE, Pozzi A, Banks SA, et al. Effect of tibial plateau leveling osteotomy on femorotibial contact mechanics and stifle kinematics. *Vet Surg* 2009;38:23-32.
22. Stauffer KD, Tuttle TA, Elkins AD, et al. Complications associated with 696 tibial plateau leveling osteotomies (2001-2003). *J Am Anim Hosp Assoc* 2006;42:44-50.
23. Pacchiana PD, Morris E, Gillings SL, et al. Surgical and postoperative complications associated with tibial plateau leveling osteotomy in dogs with cranial cruciate ligament rupture: 397 cases (1998-2001). *J Am Vet Med Assoc* 2003;222:184-193.
24. Priddy NH, 2nd, Tomlinson JL, Dodam JR, et al. Complications with and owner assessment of the outcome of tibial plateau leveling osteotomy for treatment of cranial cruciate ligament rupture in dogs: 193 cases (1997-2001). *J Am Vet Med Assoc* 2003;222:1726-1732.
25. Warzee CC, Dejardin LM, Arnoczky SP, et al. Effect of Tibial Plateau Leveling on Cranial and Caudal Tibial Thrusts in Canine Cranial Cruciate-Deficient Stifles: An In Vitro Experimental Study. *Vet Surg* 2001;30:278-286.
26. Reif U, Hulse DA, Hauptman JG. Effect of Tibial Plateau Leveling on Stability of the Canine Cranial Cruciate-Deficient Stifle Joint: An In Vitro Study. *Vet Surg* 2002;31:147-154.
27. Didia BC, Jaja BNR. Posterior Slope of Tibial Plateau in Adult Nigerian Subjects. *Int J Morphol* 2009;27:201-204.
28. Chiu KY, Zhang SD, Zhang GH. Posterior slope of tibial plateau in Chinese. *J Arthroplasty* 2000;15:224-227.
29. Bellemans J, Robijns F, Duerinckx J, et al. The influence of tibial slope on maximal flexion after total knee arthroplasty. *Knee Surg Sports Traumatol Arthrosc* 2005;13:193-196.
30. Ostermeier S, Hurschler C, Windhagen H, et al. In vitro investigation of the influence of tibial slope on quadriceps extension force after total knee arthroplasty. *Knee Surg Sports Traumatol Arthrosc* 2006;14:934-939.
31. Malviya A, Lingard E, Weir D, et al. Predicting range of movement after knee replacement: the importance of posterior condylar offset and tibial slope. *Knee Surg Sports Traumatol Arthrosc* 2009;17:491-498.

32. Varadarajan KM, Harry RE, Johnson T, et al. Can in vitro systems capture the characteristic differences between the flexion-extension kinematics of the healthy and TKA knee? *Med Eng Phys* 2009;31:899-906.
33. Zavatsky AB. A kinematic-freedom analysis of a flexed-knee-stance testing rig. *J Biomech* 1997;30:277-280.
34. Chailleux N, Chevalier Y, Hagemeister N, et al. In vitro 3-dimensional kinematic evaluation of 2 corrective operations for cranial cruciate ligament-deficient stifle. *Can J Vet Res* 2007;71:175-180.
35. Wilson DR, Feikes JD, Zavatsky AB, et al. The components of passive knee movement are coupled to flexion angle. *J Biomech* 2000;33:465-473.
36. Fu Y-C, Torres BT, Budsberg SC. Evaluation of a three-dimensional kinematic model for canine gait analysis. *Am J Vet Res* 2010;71:1118-1122.
37. Series Displacement Sensors: Microminiature DVRT. Displacement Sensors: Microminiature DVRT. Available at: <http://www.microstrain.com/displacement/dvrt>. Accessed August 7, 2012.
38. Fleming BC, Beynon BD. In Vivo Measurement of Ligament/Tendon Strains and Forces: A Review. *Ann Biomed Eng* 2004;32:318.
39. Lister SA, Renberg WC, Roush JK. Efficacy of immobilization of the tarsal joint to alleviate strain on the common calcaneal tendon in dogs. *Am J Vet Res* 2009;70:134-140.
40. Korvick DL, Pijanowski GJ, Schaeffer DJ. Three-dimensional kinematics of the intact and cranial cruciate ligament-deficient stifle of dogs. *J Biomech* 1994;27:77-87.
41. Arms SW, Pope MH, Johnson RJ, et al. The biomechanics of anterior cruciate ligament rehabilitation and reconstruction. *Am J Sports Med* 1984;12:8-18.
42. Solomonow M, Baratta R, Zhou BH, et al. The synergistic action of the anterior cruciate ligament and thigh muscles in maintaining joint stability. *Am J Sports Med* 1987;15:207-213.
43. Kain CC, McCarthy JA, Arms S, et al. An in vivo analysis of the effect of transcutaneous electrical stimulation of the quadriceps and hamstrings on anterior cruciate ligament deformation. *Am J Sports Med* 1988;16:147-152.
44. Scanlan SF, Dyrby C, Ajit M.W., Dyrby CO, et al. Differences in tibial rotation during walking in ACL reconstructed and healthy contralateral knees. *J Biomech* 2010;43:1817-1822.
45. Fregly BJ, Rahman HA, Banks SA. Theoretical accuracy of model-based shape matching for measuring natural knee kinematics with single-plane fluoroscopy. *J Biomech* 2005:692.
46. Hatfield GL, Hubley-Kozey CL, Astephen Wilson JL, et al. The effect of total knee arthroplasty on knee joint kinematics and kinetics during gait. *J Arthroplasty* 2011;26:309-318.

## CHAPTER 3

### In Vitro Kinematics of the Stifle and Gastrocnemius Tendon Strain in Three Chicken Breeds <sup>2</sup>

---

<sup>2</sup> Baker, K.B., T.L. Foutz, K.J. Johnsen, and S.C. Budsberg. To be submitted to *Poultry Science*.

### 3.1 Abstract

**Objective-** The primary objective of this study was to quantify the *in vitro* three-dimensional kinematics of the stifle of three breeds of broiler chickens with varying prevalences of leg deformities. A secondary objective was to measure the strain of the gastrocnemius (gastroc) tendon and compare stifle kinematics before and after transection of the gastroc tendon.

**Sample-** Six pelvises collected from each of three breeds of chicken that represented varying susceptibilities to leg problems: Athens-Canadian, 1996 Broiler, Commercial Broiler.

**Procedure-** Each pelvis was mounted on a modified Oxford knee rig that allowed for six degrees of freedom of the stifle while preserving the hip and hock joints. Flexion/extension was simulated while kinematic data and gastroc tendon strain were measured continuously. Kinematic data was again collected after gastroc tendon transection. Joint coordinate systems on the femur and tibia were constructed to calculate stifle kinematics in all six degrees of freedom.

**Results-** Stifle kinematics and gastroc tendon strain varied significantly among breeds. The Athens-Canadian with the lowest prevalence of leg deformities exhibited stifle kinematics similar to the human knee. The 1996 Broiler stifle showed a reversal from abduction to adduction and a decrease in internal rotation when compared to the Athens-Canadian. Gastroc tendon strain was positively correlated with the prevalence of leg deformities in a breed. As expected, transection of the gastroc tendon caused decreased flexion in all three breeds as well as a reversal in abduction/adduction in both the Athens-Canadian and Commercial Broiler.

**Conclusions-** Results from this study suggest that the kinematics of the broiler stifle are indicative of the prevalence of leg problems within a breed. In the healthy broiler stifle, the gastrocnemius tendon may serve to resist excess abduction caused by the collateral ligaments. The reversal from normal abduction to adduction in the 1996 Broiler may occur to counterbalance the increased cranially oriented bodyweight of the faster growing breed.

## 3.2 Introduction and Literature Review

### 3.2.1 Background and Importance

Musculoskeletal abnormalities in commercial broiler chickens are prevalent among various breeds and under a variety of conditions with reports of up to 90% of broilers affected.<sup>1</sup> Studies suggest that these abnormalities are due to the birds' rapid growth rate, which causes abnormally high loads to be placed on relatively immature joints.<sup>2,3</sup> While many breeds are affected, the prevalence and degree of lameness among breeds varies significantly and is attributed mainly to growth capacity determined by breeding techniques. Multiple studies have shown that leg deformities are heritable, and should therefore be preventable with careful breeding techniques.<sup>1-5</sup> Previous studies have established clinical gait scores to compare the walking abilities of broilers; however, there is no data quantifying the kinematics of the broiler gait.<sup>1</sup> Before leg problems in commercial broilers can be addressed, the source of the abnormalities must be ascertained. Comparing gait kinematics among breeds with varying degrees of leg problems will supply another quantifiable parameter of efficiency when performing selective breeding. With the incidence of broiler leg abnormalities increasing due to selective breeding for rapid growth rate, determining the causes of leg weakness in broilers will have great impact on the welfare of commercial broilers and has the potential to save the industry millions of dollars annually.

### 3.2.2 Skeletal Abnormalities in Modern Broilers

In 2011, approximately 90 billion broiler chickens were produced in the United States.<sup>6</sup> Over the past 60 years, there has been a continuous increase in market weight of domestic broilers, mainly due to genetic selection for increased breast weight for efficiency.<sup>2,7-9</sup> Growth rate more than doubled from 1960 to 2000, significantly reducing the number of days to achieve market weight.<sup>2,10,11</sup> However, increased body size and breast muscle introduce increased stresses on the immature skeletal system of the modern commercial broiler.<sup>7</sup> As a result, leg weakness has been investigated as a serious problem in fast-growing broilers.

Kestin et al.<sup>1</sup> detected gait abnormalities in 90% of broiler chickens and showed that 26% of broilers suffered an abnormality that affected their welfare. Sorensen et al.<sup>12</sup> assessed gait score and liveweight in 4,640 broilers with varying photoperiod manipulations. Results showed strong correlations between gait score and liveweight. Sanotra et al.<sup>13</sup> performed a similar study in Denmark of 2800 chicks from 28 different broiler flocks qualitatively assessing walking ability and the prevalence of leg disorders. The study revealed high incidences of impaired walking ability (75%), tibial dyschondroplasia (57%), varus/valgus deformation (37%), and crooked toes (32%).

Hocking et al.<sup>14</sup> examined over 900 commercial broilers, layers, and traditional chickens at 6, 8, and 10 weeks of age. Results showed that the commercial broilers' tibial plateau angle was 24° at 6 weeks compared to the 15° and 16° plateaus of the layer and traditional chicken respectively. While all three breeds saw an increase in plateau angle with age, the commercial broiler's plateau angle was consistently steeper than the other breeds by approximately 10°. Corr et al.<sup>15</sup> performed a study comparing random-bred and genetically-selected chickens fed both *ad-libitum* and with restricted diets. Results showed that chickens bred for rapid growth, fed *ad-libitum* had the steepest tibial plateau angle of 23°. Results also showed that the random-bred, feed-restricted birds had wider tarsometatarsal diameters than birds fed *ad-libitum*. This is thought to be due to the fact that bone development is slower during periods of rapid growth, catching up after maturity when muscle strength and bodyweight have peaked.<sup>16</sup> Since bone development is slower than muscle development, selective breeding for rapid growth tends to place abnormally high strains on bones in the leg, causing deformities and problems walking. These studies show a correlation between tibial plateau angle and the prevalence of leg deformities in the modern commercial broiler that affects the welfare of the birds.

### 3.2.3 Genetic Selection for Rapid Growth Rate

The time for a chick to reach market weight has been steadily decreasing, reduced from 120 days in 1925 to only 30 days in 2005.<sup>17</sup> It has been suggested that younger birds may be more sensitive to

liveweight than older birds due to weaker skeletal systems and that a large proportion of leg weakness is related to rapid juvenile growth rate.<sup>3,18</sup> Julian<sup>2</sup> suggests that shorter growth periods provide an insufficient amount of time for proper alignment and remodeling of bones in the leg. Tissues become stronger and more resilient with age, especially bones, tendons and ligaments, which are then better able to support naturally increased weights. Kestin et al.<sup>3</sup> investigated age differences associated with lameness in a study involving thirteen genotypes of poultry with a wide range of growth profiles and two different feeding programs. Degree of lameness was assessed qualitatively after 54 and 81 days. Results suggested that younger birds may be more sensitive to differences in weight than older birds and therefore become lamer for each unit of weight gain than older birds.

Genetic factors influencing liveweight and growth rate are important determinants of lameness in a diverse range of genotypes.<sup>1,3</sup> Skeletal causes of lameness are thought to result from the intensive genetic selection for liveweight and breast meat yield.<sup>5</sup> Kestin et al.<sup>4</sup> investigated leg weakness among different commercial broiler crosses with 2,687 chicks from four genetic lines. The gait of each bird was scored individually by an experienced assessor on a 0 to 5 scale when the birds moved spontaneously in the rearing environment. Results indicated that gait scores differ significantly among genetic lines independent of bodyweight, suggesting that improved genetic selection could decrease the high prevalence of leg deformities seen in modern broiler lines independently of live bodyweight. Havenstein et al.<sup>9</sup> investigated bodyweight, feed consumption, and mortality in a 1957 control strain and a 2001 modern strain of broilers when fed diets representative of their years. The modern strain reached market weight at 32 days while the control strain would not have reached the equivalent weight until 101 days. With the mortality rate of the control strain at half the rate of the modern strain, results showed that mortality rates and skeletal defects in broilers are rare or absent in slower growing strains.

The most significant and common developmental disorder of the broiler skeleton is varus/valgus deformation, with varus deformities resulting in more serious walking difficulty.<sup>13,19</sup> Angular bone

deformity appears to be specifically related to rapid growth, indicating that it could be reduced by slowing the growth rate during the first 10-21 days of life.<sup>2</sup> A study by Julian<sup>2</sup> also suggests that rapid growth rate leads to severe lameness, bone defects, and deformities. The risk of leg problems could be reduced by decreasing the rapid growth rate that has been shown to cause skeletal deformities.<sup>13</sup>

#### 3.2.4 Gastrocnemius Tendon Rupture

The gastroc tendon is a key contributor to the knee flexion mechanism. The medial and lateral heads of the gastrocnemius muscle originate on the posterior surface of the medial and lateral femoral condyles, merging at the gastroc tendon which inserts onto the posterior surface of the calcaneus.<sup>20</sup> Rupture of the gastroc tendon is widely recognized as a cause of lameness in broilers. It was previously thought that rupture was caused by reovirus or staphylococcus infection<sup>21,22</sup>; however, it has been hypothesized that genetic selection for increased growth rate and bodyweight contribute to the condition as well.<sup>19,23,24</sup> In a case study by Crespo et al.<sup>23</sup>, the mortality rate due to gastroc tendon rupture was 0.5% to 1% in a flock, equivalent to a loss of 60 birds per day. Post-mortem evaluation showed that infectious agents were not the cause of rupture. All tendon ruptures were observed in hens only, and were thought to be due to excess movement and jumping to avoid aggressive males after an increase in the male-to-female ratio. In a study by Dinev<sup>24</sup> of 8 broiler breeder flocks from two farms with over 10,000 broiler hens, the incidence of lameness in female birds was 4% and 8%. Rupture of the gastroc tendon accounted for the cause of lameness in 78 birds. Because of the lack of tenosynovitis or arthritis in the affected birds, this study provides evidence for spontaneous rupture of the tendon unrelated to infection. While it is clear that rupture of the gastroc tendon will affect the bird's ability to flex the stifle and therefore inhibit walking, its full effects on stifle biomechanics are unknown.

### 3.2.5 Broiler Welfare and Economic Losses

Skeletal deformities and leg problems in broiler chickens compromise the welfare of the birds.<sup>4,25</sup>

There is increasing evidence that birds with moderate leg weakness suffer from pain as they walk.

Danbury et al.<sup>26</sup> investigated 32 broilers with healthy legs and 32 lame broilers. Birds were conditioned to recognize the difference in color between two feeds: analgesic-treated and normal. The birds were then individually housed and allowed to feed *ad-libitum* with a choice of feed. At the end of the self-selection period, blood samples were taken and walking ability of each bird was reassessed. Results showed that both lame and healthy broilers consumed the same amount of feed, but the lame birds included significantly more of the drugged feed in their diet, which increased with degree of lameness.

These findings support the hypothesis that broilers with lameness experience pain, which causes distress from which they seek relief. Similarly, Weeks et al.<sup>27</sup> investigated the number of visits to the feeder as related to leg weakness. Following 4 hours of food withdrawal, 40 broilers each with good and poor walking ability were given access to a feeder. Results indicated that lame birds visit the feeder significantly less frequently than healthy birds. Assuming that all birds had the same high motivation to feed, the results indicated that birds experiencing lameness had a conflicting need to remain lying, which sometimes took preference over feeding.

Leg weakness was estimated to cause a mortality rate of 3.2% of the total US broiler population in 1993, which cost the broiler industry an estimated \$80-120 million.<sup>19,28</sup> With the growth rate currently greater than that of 1993, increased incidence of leg weakness and greater economic loss is expected in today's broiler industry.

### 3.2.6 Gait Score and Stifle Kinematics

The stifle joint moves through complex kinematic motions during the gait cycle with six degrees of freedom clinically described by three rotations (flexion/extension, adduction/abduction, internal/external) and three translations (cranial/caudal, medial/lateral, proximal/distal) shown in Figure

3.1. Currently, experienced researchers commonly assess walking ability in commercial broilers visually with a method developed by Kestin et al.<sup>1</sup> involving a 0 to 5 scale. This method is effective at evaluating a bird's ability to walk, but says little about the type or cause of lameness of the bird. This method also requires an experienced researcher to perform the assessment and is subject to variations between examiners. The method does not attempt to describe the motions of the stifle, but only evaluates a bird's ability to walk. Measuring the kinematics of the stifle in all six degrees of freedom is a more objective and quantifiable way of identifying and categorizing leg problems that could standardize the diagnosis of various types of leg problems seen in the modern broiler. Comparing the stifle kinematics of a lame versus a healthy broiler may also help determine the causes behind leg weakness.

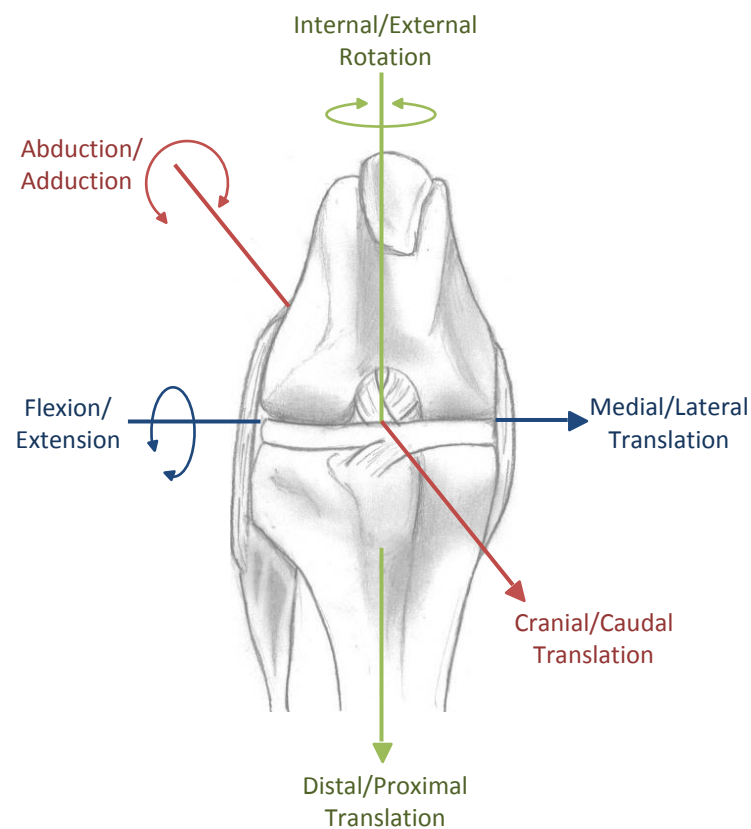


Figure 3.1: The six degrees of freedom of the stifle, clinically described as three rotations (flexion/extension, internal/external, abduction/adduction) and three translations (cranial/caudal, medial/lateral, proximal/distal).

### 3.2.7 The Oxford Knee Rig

The kinematics of the human knee have been researched extensively both *in vitro* and *in vivo* to map its natural motions. *In vivo* studies more fully represent physiological conditions, which are impossible to replicate fully with cadaveric studies. However, an advantage to *in vitro* systems is that test conditions are more easily altered and evaluated within specimens, minimizing variability among specimens.<sup>29</sup> To simulate the natural kinematic motions of the stifle in a cadaveric hind limb, the knee must travel through all six degrees of freedom. Experimental testing with knee simulators is often used to quantitatively evaluate the performance of specific treatments on the kinematics of the human knee joint.<sup>30</sup> The most commonly used simulator for kinematic testing is the Oxford Knee Rig (OKR) which was first designed by Bourne et al.<sup>31</sup> to test post-mortem human knee joints by allowing for six degrees of freedom of the stifle joint during a deep flexion stance.

There have been multiple studies published using similar knee kinematic testing devices to investigate the effects of different surgical treatments on the kinematics of the human knee. Bellemans et al.<sup>32</sup> simulated deep flexion in 21 human cadaver legs before and after a standard TKR with tibial plateau angles ranging from 0° to 7°. Results showed an average gain of 1.7 degrees flexion for every degree of tibial slope. Similarly, Ostermeier<sup>33</sup> measured implant displacement and the quadriceps force required to extend the knee in seven cadaveric specimens after total knee replacement with tibial plateau angles of 0° and 10°. Results showed a significant difference between the two treatments with the posterior slope causing more physiologic insert movement and reduced quadriceps force.

In a review of OKR studies involving human cadaver legs, Varadarajan et al.<sup>29</sup> concluded that the OKR can replicate femoral rollback and the screw home mechanism between 0° and 30° flexion, and also reduced femoral rollback and an absence of the screw home mechanism in TKR patients. It was suggested that the OKR's ability to replicate internal rotation of the knee beyond 30° was inconsistent among studies, and that results should be carefully interpreted. Yildirim et al.<sup>34</sup> simulated deep flexion

with a rig that pulled the quadriceps tendon utilizing springs to simulate the hamstrings. Seven cadaver knees were run intact, after ACL transection, and after implantation with four different types of TKR's. The path of the articulating surfaces was mapped for each treatment, and significant differences were shown between treatments in axial rotation and mediolateral displacement. Kondo et al.<sup>35</sup> used an optical tracking system to track eight cadaver legs mounted on an OKR to test the difference between knees before and after ACL transection and single- and double-bundle ACL reconstructions. Significant differences in kinematics were found between the treatments for internal rotation and craniocaudal translation.

While many of these studies have used the OKR to drive the motion of a cadaveric specimen with only the quadriceps retained, it has been shown that such techniques can cause a distortion in the joint's natural kinematics because the removal of muscle groups results in a loss of the muscle tensions and constraints placed across the joint.<sup>36</sup> Varadarajan et al.<sup>29</sup> suggest that the inclusion of muscle provides more physiological constraints which provide important implications with regards to the ability of the OKR to simulate natural knee motions. Wilson et al.<sup>37</sup> found that in cadaveric knees flexed passively without simulating muscle forces, internal/external rotation, abduction/adduction, and all three components of translation are coupled to flexion/extension angle in the normal knee. This suggests that passive knee motion is guided by articular contact in the medial and lateral compartments and the passive constraints of the surrounding ligaments. These studies have shown that simulating deep flexion in human cadaver legs with an Oxford knee rig can detect significant differences in kinematics between various treatments. Therefore, similar techniques should be able to detect differences in the kinematics of broilers with varying leg deformities.

### 3.3 Purpose of Study

The primary purpose of this study was to characterize the kinematic motion of the stifle in three breeds of broiler chickens by simulating deep flexion in cadaver limbs. A secondary objective was to

determine the function and strain of the gastroc tendon of each broiler breed during deep flexion. The questions of interest were: (1) was there significant variability in kinematics between the three breeds; (2) was there significant variability in strain to the gastroc tendon between the three breeds; and (3) were there significant differences in kinematics within breeds after gastroc tendon transection.

Understanding how joint motions differ between breeds will provide important information about how breeding for rapid growth rate affects stifle kinematics. This will provide an important basis for improvements to breeding techniques, leading to greater quality of life for commercial broilers.

### 3.4 Materials & Methods

#### 3.4.1 Samples and Preparation

Three breeds of birds were chosen to represent varying prevalences of leg deformities. Athens-Canadians were used to represent a slower growing bird with relatively minimal leg problems compared to commercial broilers. 1996 Broilers were used to represent a bird with a history of moderate leg problems. Commercial Broilers, which have a history of a high prevalence of leg deformities, were chosen to represent a condition common to industry. Six birds each from the 1996 Broiler line and a Commercial Broiler line were sacrificed at six weeks of age. Six Athens-Canadians were sacrificed after reaching sexual maturity (approximately 21 weeks old). Specimens were prepared by detaching the legs and spine from the main body and removing all skin above the tarsal joint while preserving all musculature. Specimens were stored at  $-40^{\circ}\text{C}$  and taken out to thaw four hours in advance of testing.

#### 3.4.2 Simulated Motion Cycle

The spine of each bird was attached to a modified OKR with two bolts while the feet were held rigid on a horizontal platform (Figure 3.2). The modified OKR simulates passive flexion and extension in a cadaveric leg by controlling vertical motion of the spine. The rig allows for all six degrees of freedom of the stifle through horizontal sliders mounted in the craniocaudal and mediolateral planes. The spinal

attachment was mounted on a clevis hanger to allow the spine to freely rotate in the craniocaudal plane to simulate the natural motion of the spine during squatting in a live bird. Kirschner wire (1.6 mm diameter) was drilled into the bone at 6 anatomical locations, and reflective markers were attached to the end of each wire at the surface of the skin. Prior to testing, the stifle and hock joints were moved through a full range of motion to ensure no impingement from the wires. Each specimen underwent five motion cycles from full extension to full flexion (130-85°) while kinematic and strain data were collected.

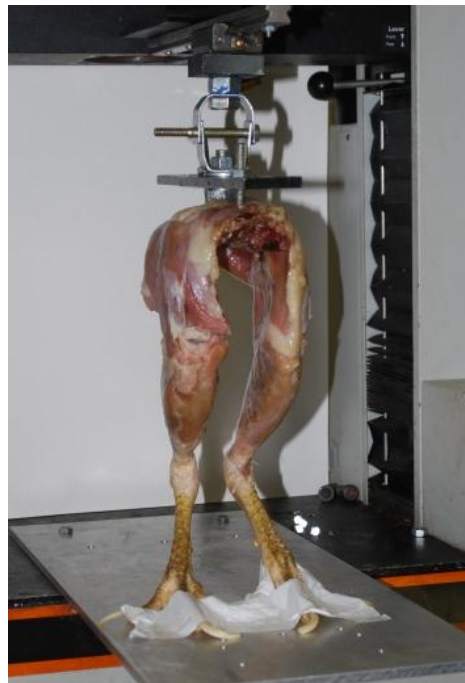


Figure 3.2: The modified Oxford knee rig simulates flexion/extension by holding the feet rigid while moving the spine vertically, allowing for six degrees of freedom of the stifle.

### 3.4.3 Motion Tracking

During the motion cycle, three-dimensional marker positions were collected with a set of five Vicon T-series infrared cameras at 200 Hz with Vicon Motus software. The reflective markers and wires remained in place throughout the duration of the experiment. Using the raw marker locations, the angular and translational motions of the stifle joint were calculated in Matlab using the joint coordinate system technique described by Fu et al.<sup>38</sup> (Figure 3.3). Rotations about the three clinical axes were

calculated and reported as motion of the tibia relative to the femur. Kinematic motions except flexion/extension were calculated in reference to the initial position at full extension with an angle of  $0^\circ$  or a translation of 0 mm indicating the joint was in the same orientation as the initial frame at full extension. Translations were calculated from tibial crest to the midpoint of the femoral epicondyles along the long femoral axis.

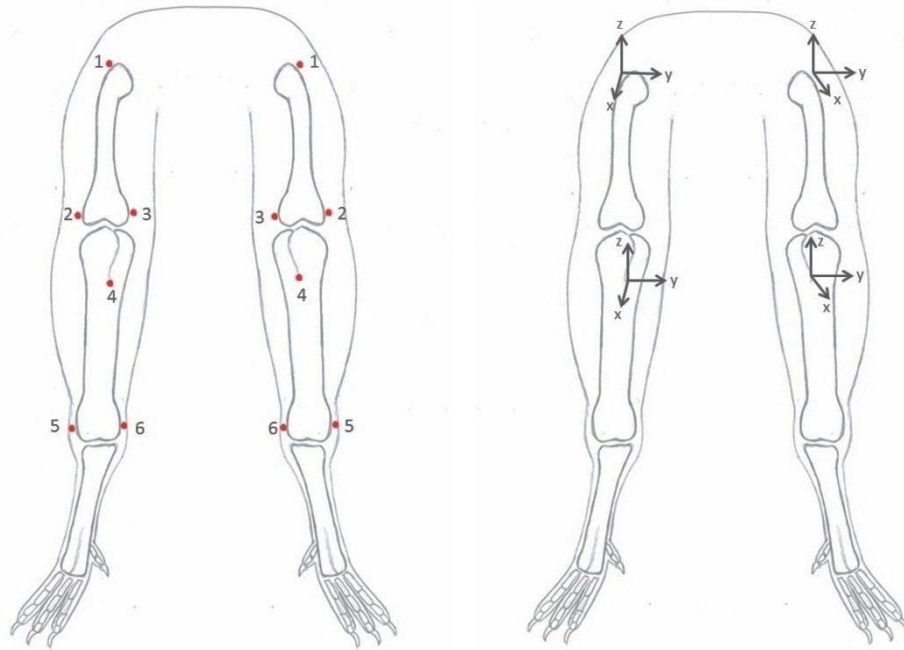


Figure 3.3: Cranial view of the hind limbs of a chicken with reflective marker k-wire locations shown in red (left) and the constructed Joint Coordinate Systems located on the greater trochanter and tibial crest for the femur and tibia respectively (right). Markers locations: 1-greater trochanter, 2-lateral epicondyle, 3-medial epicondyle, 4-tibial crest, 5-lateral malleolus, 6-medial malleolus. Joint coordinate system axes: x +cranial; y +lateral left leg/+medial right leg; z +proximal.

#### 3.4.4 Gastrocnemius Tendon Strain

The displacement of the gastroc tendon was measured during the motion cycle. A displacement sensor (MicroStrain, M-DVRT-3) was attached to the gastroc tendon using barbs on the sensor. The long axis of the sensor was aligned to the long axis of the tendon with the specimen was at full extension. Displacement was calculated from the output voltages using the factory calibrated polynomial fit

equations. Strain on the tendon was calculated as the ratio of sensor displacement to original length between the barbs. The displacement sensor is comprised of a main body and freely moving core that detects core position by measuring the coils differential reluctance using a sine wave excitation and synchronous demodulator (Figure 3.4).<sup>39-41</sup> The sensor was connected directly to a signal conditioner (MicroStrain, DEMOD-DVRT) calibrated at the factory with the sensor. A Vernier LabPro Data Logger and computer with software (Logger Pro 3.6.0) were used to collect the conditioned output voltage from the displacement sensor at 200 Hz.

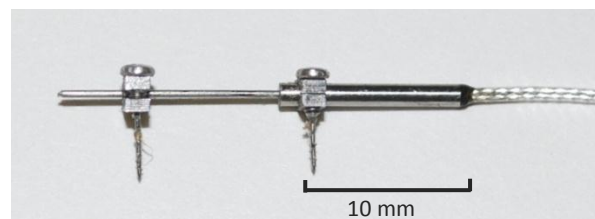


Figure 3.4: MicroStrain 3 mm displacement sensor (M-DVRT-3) with barbs.

#### 3.4.5 Experimental Procedure

Each specimen was mounted to the modified OKR with the gastroc tendon intact and run for five cycles as previously described while collecting kinematic data. Two subsequent trials were run first with the periosteum over the gastroc tendon severed, then with the displacement sensor attached to the gastroc tendon to collect displacement data. Kinematic data was collected during both trials to determine if severing the periosteum and attaching the sensor altered the kinematics of the stifle. The displacement sensor was subsequently removed and the gastroc tendon severed. Each specimen was run through five cycles through the same range of motion as the initial trial (i.e. range of motion of was not adjusted to reach identical flexion/extension angles after each treatment).

Tibiae and femurs from each specimen were dissected out with the stifle joint ligaments intact. Lengths of the collateral and cruciate ligaments were measured from origin to insertion, and width was measured at the mid-length point. Length and mid-diaphyseal width of the tibiae and femurs were

measured in the mediolateral plane. The joint was disarticulated and the menisci and ligaments removed from the tibia. Medial view images were taken of the proximal end of the tibia, and tibial plateau angles were drawn and measured. Plateau angle was measured as the angle between (a) the long axis of the femur drawn from the midpoint of the intercondylar eminences to the center of the tarsal joint; and (b) the medial tibial plateau drawn from the proximal tibia's most cranial to caudal margins.

#### 3.4.6 Statistical Analysis

For all kinematics and gastroc tendon strain, peak range of motion and strain for each cycle was calculated and compiled for each treatment. The questions of interest were: was there significant variability in kinematics and gastroc strain (a) between the three breeds of broilers, and (b) within each breed after each subsequent treatment. All statistical analyses were calculated in Minitab (release 13 for Windows). Using the compiled peak range of motion and peak strain data, a one-way ANOVA was used to compare significant differences in kinematic and strain data between breeds. Where significant differences were indicated, paired comparisons were made using a post hoc Tukey's test. The same procedure was repeated to determine if there were differences within breeds between the normal stifle and the following three treatments: (1) periosteum severed, (2) displacement sensor attached, and (3) gastroc tendon severed. A significance level of  $p < 0.05$  was used for all analyses.

### 3.5 Results

#### 3.5.1 Normal Stifle Kinematics and Gastroc Tendon Strain

A summary of mean peak kinematics of the tibia relative to the femur and strain values is shown in Table 3.1 and Figures 3.5-3.6. Adduction varied significantly between all breeds. Internal rotation varied significantly between the Athens-Canadian and the 1996 Broiler. There were no significant differences in internal rotation between the Commercial Broiler and either other breed. Medial translation varied

significantly between the Commercial Broiler and both the Athens-Canadian and 1996 Broiler. There was no significant difference in medial translation between the Athens-Canadian and the 1996 Broiler. There were no significant differences between breeds in caudal or distal translation. Peak values of strain were significantly different between all breeds.

Table 3.1: Mean Peak Kinematics and Gastroc Tendon Strain by Breed.  
Kinematics are reported as motion of the tibia relative to the femur during flexion.  
Rotations/translations within a column with different superscripts are significantly different ( $p < 0.05$ ).

|                       |      | Rotations (degrees)       |                         | Translations (mm)    |                      |                       | Strain (%)        |
|-----------------------|------|---------------------------|-------------------------|----------------------|----------------------|-----------------------|-------------------|
|                       |      | +Adduction/<br>-Abduction | +External/<br>-Internal | +Cranial/<br>-Caudal | +Lateral/<br>-Medial | +Proximal/<br>-Distal |                   |
| Athens-<br>Canadian   | Mean | -3.6 <sup>a</sup>         | -16.0 <sup>a</sup>      | -11.4                | -7.4 <sup>a</sup>    | -11.9                 | 0.55 <sup>a</sup> |
|                       | ±SD  | 0.1                       | 6.3                     | 4.9                  | 0.4                  | 0.8                   | 0.14              |
| 1996 Broiler          | Mean | +9.2 <sup>b</sup>         | -11.5 <sup>b</sup>      | -12.1                | -7.0 <sup>a</sup>    | -10.7                 | 2.42 <sup>b</sup> |
|                       | ±SD  | 5.2                       | 3.2                     | 4.6                  | 3.2                  | 3.3                   | 0.79              |
| Commercial<br>Broiler | Mean | +2.8 <sup>c</sup>         | -10.2 <sup>ab</sup>     | -13.0                | -2.3 <sup>b</sup>    | -10.4                 | 7.00 <sup>c</sup> |
|                       | ±SD  | 4.3                       | 7.4                     | 3.9                  | 3.5                  | 3.2                   | 2.68              |

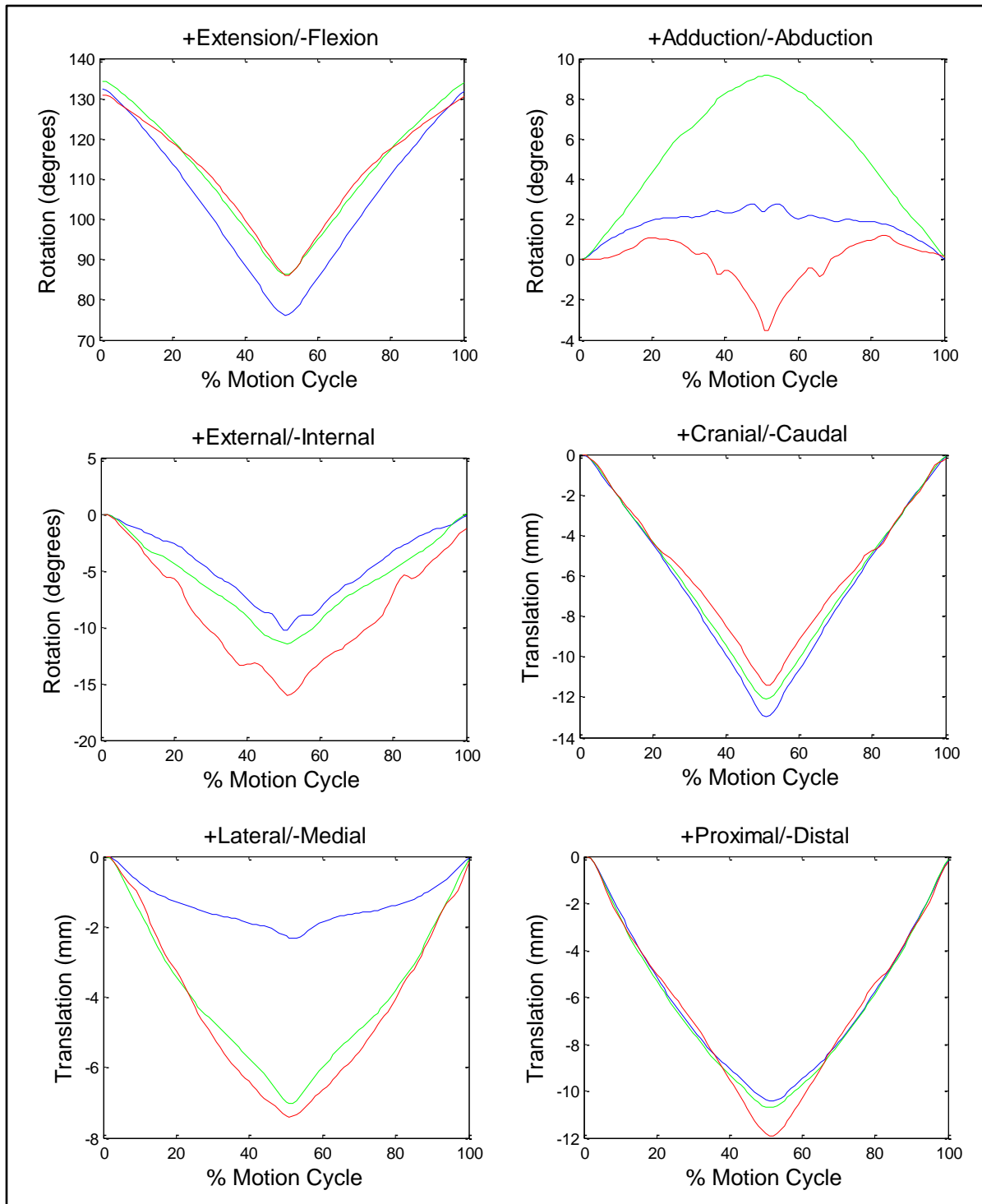


Figure 3.5: Comparison of Mean Kinematics of Intact Broiler Stifles. Percent motion cycle starts and ends at full extension (130°) with full flexion (85°) at 50% motion cycle. All kinematics are reported as motion of the tibia relative to the femur. Red- Athens-Canadian, Green- 1996 Broiler, Blue- Commercial Broiler

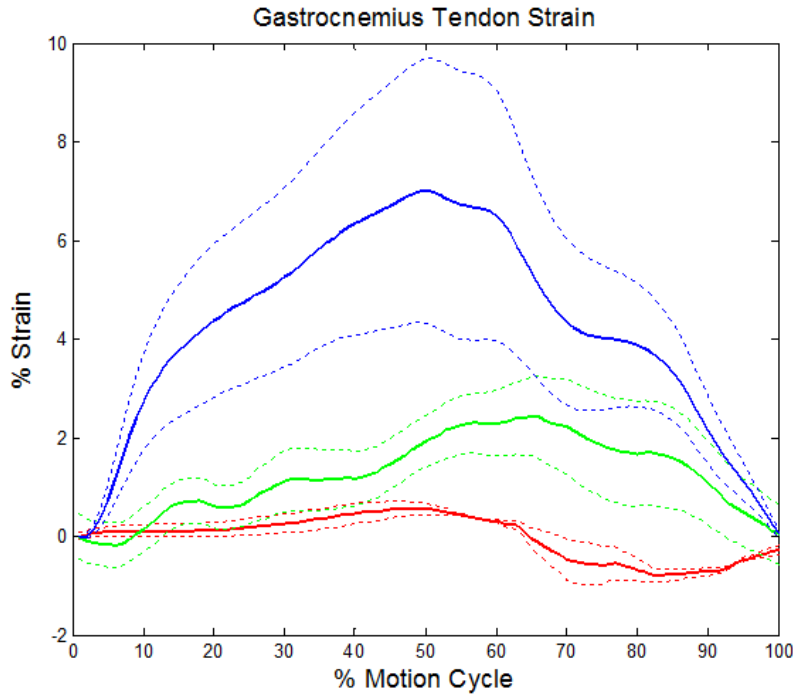


Figure 3.6: Mean Gastroc Tendon Strain by Breed. Percent motion cycle starts and ends at full extension (130°) with full flexion (85°) at 50% motion cycle. 95% confidence intervals are shown as dashed lines. Red- Athens-Canadian, Green- 1996 Broiler, Blue- Commercial Broiler

### 3.5.2 Stifle Kinematics After Gastroc Tendon Transection

There were no significant changes in kinematics after severing the periosteum over the gastroc tendon or attaching the displacement sensor.

A summary of all mean peak kinematic values with standard deviations before and after gastroc tendon transection is shown in Table 3.2 and Figures 3.7-3.9. After transection of the gastroc tendon, the Athens-Canadian stifle showed significant differences in extension, adduction, and distal translation. Loss of the gastroc tendon resulted in 7.3° less flexion and 1.5 mm less distal tibial translation. Abduction reversed after gastroc transection from 3.6 ± 0.1° abduction initially to 2.6 ± 1.4° adduction. The only significant difference in the kinematics of the 1996 Broiler before and after transection of the gastroc tendon was a decrease in flexion of 6.4°. The Commercial Broiler stifle showed significant

differences in extension and adduction after transection. Loss of the gastroc tendon caused 8.7° less flexion and caused a reversal from 2.8 ± 4.3° adduction to 1.2 ± 1.0° abduction.

Table 3.2: Mean Peak Kinematics Before and After Severing the Gastroc Tendon.

Kinematics are reported as motion of the tibia relative to the femur during flexion.

\* indicates significant differences between kinematics before and after transection of the gastrocnemius tendon within a breed.

|                                       |      | Rotations (degrees)     |                           |                         | Translations (mm)    |                      |                       |
|---------------------------------------|------|-------------------------|---------------------------|-------------------------|----------------------|----------------------|-----------------------|
|                                       |      | +Extension/<br>-Flexion | +Adduction/<br>-Abduction | +External/<br>-Internal | +Cranial/<br>-Caudal | +Lateral/<br>-Medial | +Proximal/<br>-Distal |
| Athens-Canadian<br>Normal             | Peak | -86.1*                  | -3.6*                     | -16.0                   | -11.4                | -7.4                 | -11.9*                |
|                                       | ±SD  | 1.0                     | 0.1                       | 6.3                     | 4.9                  | 0.4                  | 0.8                   |
| Athens-Canadian<br>Gastroc Severed    | Peak | -93.4*                  | +2.6*                     | -15.3                   | -10.4                | -7.7                 | -10.4*                |
|                                       | ±SD  | 0.2                     | 1.4                       | 5.1                     | 6.4                  | 0.5                  | 1.3                   |
| 1996 Broiler<br>Normal                | Peak | -86.3*                  | +9.2                      | -11.5                   | -12.1                | -7.0                 | -10.7                 |
|                                       | ±SD  | 2.5                     | 5.2                       | 3.2                     | 4.6                  | 3.2                  | 3.3                   |
| 1996 Broiler<br>Gastroc Severed       | Peak | -92.7*                  | +10.6                     | -11.8                   | -12.1                | -7.4                 | -9.4                  |
|                                       | ±SD  | 3.6                     | 5.0                       | 3.4                     | 4.5                  | 3.9                  | 2.9                   |
| Commercial Broiler<br>Normal          | Peak | -76.2*                  | +2.8*                     | -10.2                   | -13.0                | -2.3                 | -10.4                 |
|                                       | ±SD  | 1.7                     | 4.3                       | 7.4                     | 3.9                  | 3.5                  | 3.2                   |
| Commercial Broiler<br>Gastroc Severed | Peak | -84.9*                  | -1.2*                     | -11.1                   | -14.7                | -1.4                 | -9.0                  |
|                                       | ±SD  | 1.9                     | 1.0                       | 6.3                     | 4.2                  | 2.7                  | 2.8                   |

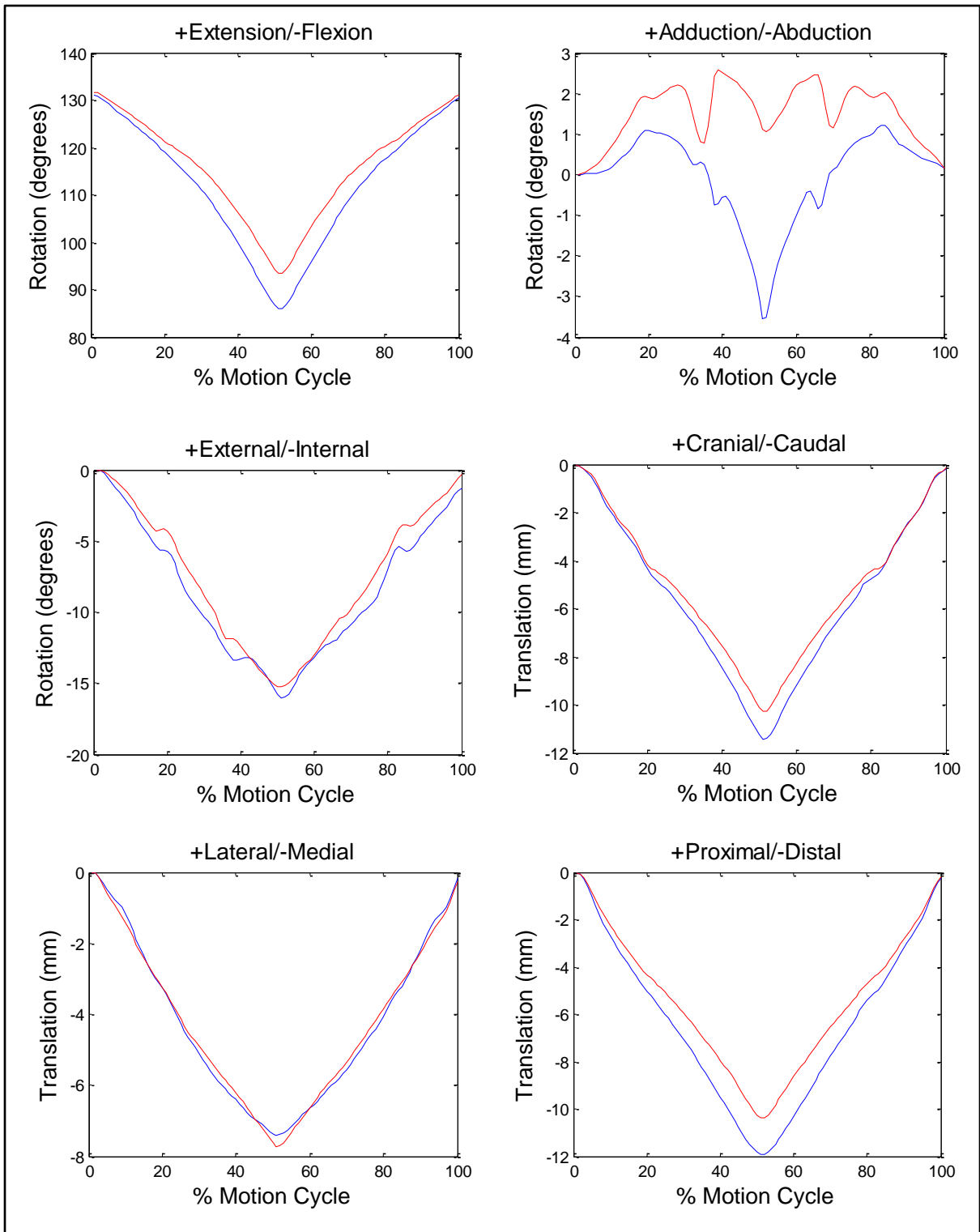


Figure 3.7: Comparison of Mean Kinematics of Normal vs Gastroc Severed Stifles in the Athens-Canadian. Percent motion cycle starts and ends at full extension (130°) with full flexion (85°) at 50% motion cycle. All kinematics are reported as motion of the tibia relative to the femur. Blue- normal, Red- gastroc tendon severed

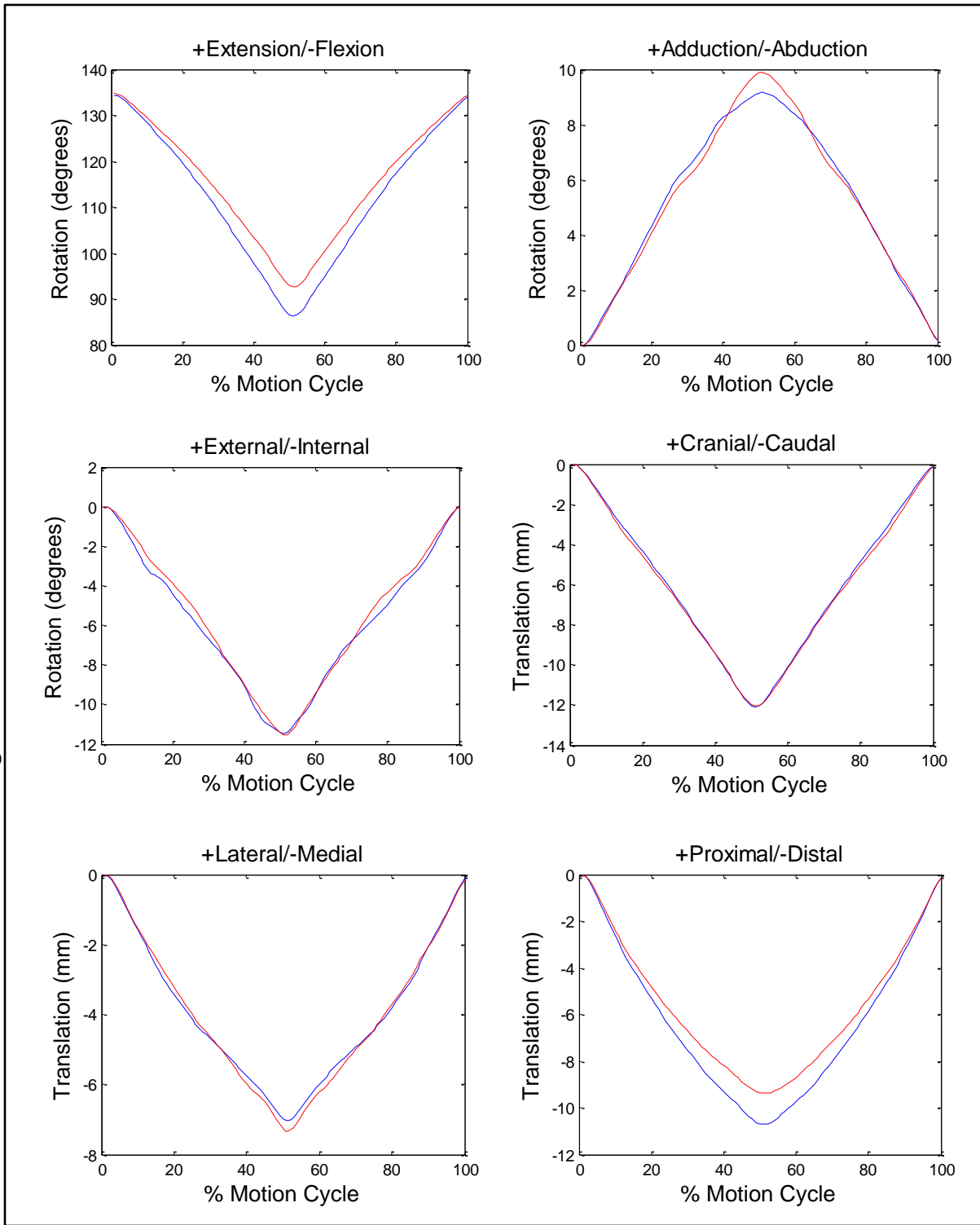


Figure 3.8: Comparison of Mean Kinematics of Normal vs Gastroc Tendon Severed Stifles in the 1996 Broiler. Percent motion cycle starts and ends at full extension (130°) with full flexion (85°) at 50% motion cycle. All kinematics are reported as motion of the tibia relative to the femur. Blue- normal, Red- gastroc tendon severed

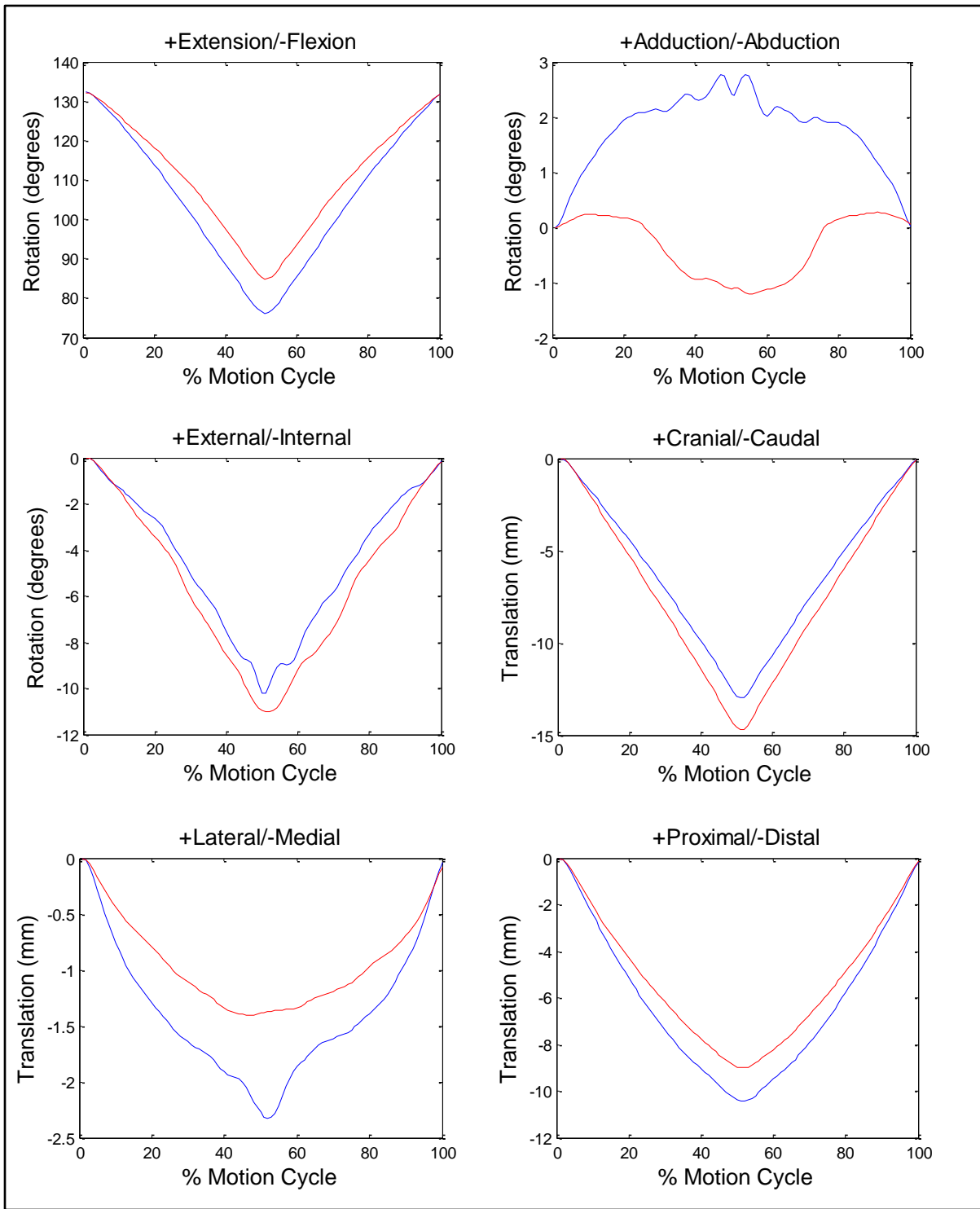


Figure 3.9: Comparison of Mean Kinematics of Normal vs Gastroc Tendon Severed Stifle in the Commercial Broiler. Percent motion cycle starts and ends at full extension (130°) with full flexion (85°) at 50% motion cycle. All kinematics are reported as motion of the tibia relative to the femur. Blue- normal, Red- gastroc tendon severed

### 3.5.3 Morphometric Measurements

A summary of all mean stifle ligament and bone measurements with standard deviations is shown in Table 3.3. There were no significant differences among breeds in MCL length, LCL length, CrCL width, or tibia width. The Athens-Canadian MCL width was significantly larger than that of the other breeds by an average of 3.48 mm. The 1996 Broiler LCL width was significantly larger than in the other breeds by an average of 3.89 mm. The Commercial Broiler CrCL length was significantly larger than that of the Athens-Canadian by 3.24 mm. The 1996 Broiler CaCL length was significantly larger than that of the Commercial Broiler by 2.06 mm. The Commercial Broiler CaCL width was significantly larger than that of the 1996 Broiler by 0.80 mm.

The lengths of the femur and tibia of the Athens-Canadian were significantly larger than in the other breeds by an average of 14.34 mm and 22.63 mm respectively. The width of the femur of the Commercial Broiler was significantly larger than that of the 1996 Broiler by 0.96 mm. The tibial plateau angle of the Commercial Broiler was significantly larger than that of the other breeds by an average of 7.7°.

Table 3.3: Morphometric Measurements of the Stifle Joint by Breed.

Length (L) and width (W) reported in mm. Tibial plateau angle (TPA) reported in degrees. MCL- medial collateral ligament; LCL- lateral collateral ligament; CrCL- cranial cruciate ligament; CaCL- caudal cruciate ligament. Mean values within a row with different superscripts are significantly different ( $p < 0.05$ ).

|       |   | Athens-Canadian     |      | 1996 Broiler        |      | Commercial Broiler  |      |
|-------|---|---------------------|------|---------------------|------|---------------------|------|
|       |   | Mean                | ±SD  | Mean                | ±SD  | Mean                | ±SD  |
| MCL   | L | 30.92               | 2.96 | 26.16               | 4.58 | 26.46               | 3.23 |
|       | W | 9.33 <sup>a</sup>   | 0.74 | 6.20 <sup>b</sup>   | 0.21 | 5.50 <sup>b</sup>   | 1.04 |
| LCL   | L | 20.68               | 1.81 | 21.22               | 2.53 | 17.87               | 3.91 |
|       | W | 3.31 <sup>a</sup>   | 0.17 | 7.22 <sup>b</sup>   | 1.87 | 3.36 <sup>a</sup>   | 0.48 |
| CrCL  | L | 9.27 <sup>a</sup>   | 0.40 | 10.67 <sup>ab</sup> | 0.88 | 12.51 <sup>b</sup>  | 1.24 |
|       | W | 3.30                | 0.07 | 3.44                | 0.20 | 3.34                | 0.80 |
| CaCL  | L | 11.18 <sup>ab</sup> | 0.38 | 12.41 <sup>a</sup>  | 0.65 | 10.35 <sup>b</sup>  | 1.12 |
|       | W | 3.15 <sup>ab</sup>  | 0.33 | 3.09 <sup>a</sup>   | 0.31 | 3.89 <sup>b</sup>   | 0.42 |
| Femur | L | 88.02 <sup>a</sup>  | 1.74 | 73.34 <sup>b</sup>  | 1.91 | 74.01 <sup>b</sup>  | 4.72 |
|       | W | 9.56 <sup>ab</sup>  | 0.82 | 8.26 <sup>a</sup>   | 0.40 | 9.22 <sup>b</sup>   | 0.47 |
| Tibia | L | 122.33 <sup>a</sup> | 0.68 | 98.57 <sup>b</sup>  | 0.99 | 100.82 <sup>b</sup> | 6.70 |
|       | W | 8.48                | 0.44 | 8.75                | 0.50 | 9.46                | 0.69 |
| TPA   |   | 20.7 <sup>a</sup>   | 1.25 | 18.8 <sup>a</sup>   | 1.30 | 27.4 <sup>b</sup>   | 3.6  |

### 3.6 Discussion

No previously published data on broiler stifle kinematics were found; therefore, results from human studies were used to compare with the results herein. Results from an *in vitro* study by Wilson et al.<sup>37</sup> with 15 human cadaveric limbs showed that human knees undergoing passive flexion exhibit -9 to +9° abduction, 14-36° internal rotation, 20-34 mm caudal tibial translation, 2-9 mm medial tibial translation, and 6-24 mm proximal tibial translation. The Athens-Canadian stifle herein was flexed passively and exhibited kinematic rotations and translations similar to results from *in vitro* human studies with the exception of proximal translation. The similarities between the kinematics of the human knee and the Athens-Canadian stifle suggest that the stifle of a healthy broiler appears similar to the human knee.

The kinematics of the 1996 Broiler significantly varied from the Athens-Canadian in both adduction and internal rotation. During flexion, the Athens-Canadian stifle showed abduction, while the 1996 Broiler stifle showed a reversal to adduction. The 1996 Broiler stifle also exhibited less internal rotation than that of the Athens-Canadian. A change from abduction to adduction is expected in faster growing birds because of increased bodyweight. A bird with larger pectoralis major muscles would be expected to have a center of mass more cranially and medially oriented than in a normal bird. This increased weight might need to be counterbalanced for stable standing and walking. By rotating the stifle joint in adduction versus abduction during flexion, the joint may act to balance the increased weight. This shift in adduction may also explain the decrease in internal rotation needed to stabilize the joint motion. With the stifle shifting to adduction, this movement may compensate for the larger degree of internal rotation seen in the Athens-Canadian.

Overall, the kinematic results from the Commercial Broiler stifle were less consistent between birds than results from the other two breeds. The larger standard deviations within the Commercial Broiler only allowed for significant difference in kinematics from the Athens-Canadian to be shown in medial translation with the Commercial Broiler exhibiting 4.8 mm less medial translation than the Athens-

Canadian. The inconsistency between kinematics and the large variations in rotations and translations within the breed may be a result of the high prevalence of leg abnormalities in Commercial Broilers.

Strain on the gastroc tendon was lowest in the Athens-Canadian and significantly larger in the 1996 Broiler and Commercial Broiler. The gastroc tendon of the Commercial Broiler exhibited the highest strain during passive flexion with a mean peak value more than ten times that of the Athens-Canadian. It is probable that the abnormal kinematics at the stifle cause the tendon to pull abnormally and contribute to the higher strains observed. After transection of the gastroc tendon, the stifle of all three breeds exhibited less flexion as the spine moved through the same range of motion as the initial trial. A smaller range of motion after gastroc transection is expected because the gastroc is a key contributor to the extensor mechanism.

The Athens-Canadian stifle also showed significantly less distal tibial translation after gastroc transection. Both the 1996 Broiler and the Commercial Broiler also showed less distal tibial translation after gastroc transection, but neither were significant. Changes in peak distal tibial translation may be attributed to the decreased range of motion after transection. Once normalized with flexion angle, there were no significant differences in distal translation before and after gastroc removal in any breed.

After severing the gastroc tendon in the Athens-Canadian, abduction reversed to adduction. These results indicate that the gastrocnemius resists adduction in a normal bird. The medial collateral ligament is less flexible than its lateral counterpart due to its attachment to the medial meniscus, inhibiting abduction and facilitating adduction at the stifle.<sup>20</sup> In the normal Athens-Canadian, the gastrocnemius counteracts the effects of the collateral ligaments, stabilizing the kinematics of the stifle joint. Severing the gastroc tendon in the Commercial Broiler caused the opposite effect seen in the Athens-Canadian. After transection, adduction in the intact stifle reversed to abduction. These results suggest that in the Commercial Broiler, with a high prevalence of leg deformities, the gastrocnemius serves to resist the abnormal excess abduction instead of adduction.

Results from the study herein showed that the femur and tibia of the Athens-Canadian were significantly longer than the other breeds. Since bone development is inhibited during periods of rapid muscle growth, it follows that chickens genetically selected for rapid growth rates like the 1996 Broiler and the Commercial Broiler would have less bone development compared to more traditional breeds.<sup>20</sup> The Commercial Broiler also had a significantly steeper tibial plateau angle, 7.7° steeper than the other two breeds. These results are similar to results from the previously mentioned studies by Hocking et al.<sup>14</sup> and Corr et al.<sup>15</sup> in which birds selectively bred for rapid growth had significantly higher tibial plateau angles than their random-bred counterparts. Results suggest that steeper plateau angles are correlated to abnormal stifle kinematics and have been linked to less stable biomechanics at the knee in many animals.

### 3.7 Conclusion

Results from this study suggest that the kinematics of the broiler stifle are indicative of the prevalence of leg problems within a breed. The breed with the lowest prevalence of leg deformities exhibited motions at the stifle similar to the human knee, with faster growing breeds deviating from the normal kinematics in abduction, internal rotation, and medial translation. It is likely that the deviation from normal stifle kinematics is due to the genetic selection for faster growth rates, leading to immature tendons, ligaments, and bone compensating for increased bodyweights. Results also suggest that abnormal kinematics significantly affect function and strain of the gastroc tendon, possibly leading to the higher occurrence of gastroc tendon rupture in faster growing breeds. In addition, results support the correlation between steeper tibial plateau angle and prevalence of leg deformities that has been seen in previous studies. These results may be used as a basis for future studies when examining the kinematics of various breeds of broilers to determine the genetic and environmental causes of leg deformities.

### 3.8 References

1. Kestin SC, Knowles TG, Tinch AE, et al. Prevalence of leg weakness in broiler chickens and its relationship with genotype. *Vet Rec* 1992;131:190-194.
2. Julian RJ. Rapid growth problems: ascites and skeletal deformities in broilers. *Poult Sci* 1998;77:1773-1780.
3. Kestin SC, Gordon S, Su G, et al. Relationships in broiler chickens between lameness, liveweight, growth rate and age. *Vet Rec* 2001;148:195-197.
4. Kestin SC, Su G, Srensen P. Different commercial broiler crosses have different susceptibilities to leg weakness. *Poult Sci* 1999;78:1085-1090.
5. Webster J. *Animal welfare: a cool eye towards Eden*. Oxford; Cambridge, Mass.: Blackwell Science, 1995.
6. Series Broiler Chicken Industry Key Facts. Broiler Chicken Industry Key Facts. Available at: <http://www.nationalchickencouncil.org/about-the-industry/statistics/broiler-chicken-industry-key-facts/>. Accessed January 17, 2012,
7. Talaty PN, Hester PY, Katanbaf MN. Bone mineralization in male commercial broilers and its relationship to gait score. *Poult Sci* 2010;89:342-348.
8. Buyse J, Michels H, Vloeberghs J, et al. Energy and protein metabolism between 3 and 6 weeks of age of male broiler chickens selected for growth rate or for improved food efficiency. *Br Poult Sci* 1998;39:264-272.
9. Havenstein GB, Ferket PR, Qureshi MA. Growth, livability, and feed conversion of 1957 versus 2001 broilers when fed representative 1957 and 2001 broiler diets. *Poult Sci* 2003;82:1500-1508.
10. Nicholson D. Research: Is it the broiler industry's partner into the new millennium? *Worlds Poult Sci J* 1998;54:271-278.
11. Sulistiyanto B, Akiba Y, Sato K. Energy utilisation of carbohydrate, fat and protein sources in newly hatched broiler chicks. *Br Poult Sci* 1999;40:653-659.
12. Sorensen P, Su G, Kestin SC. The effect of photoperiod:scotoperiod on leg weakness in broiler chickens. *Poult Sci* 1999;78:336-342.
13. Sanotra GS, Lund JD, Ersboll AK, et al. Monitoring leg problems in broilers: a survey of commercial broiler production in Denmark. *Worlds Poult Sci J* 2001;57:55-69.
14. Hocking PM, Sandercock DA, Wilson S, et al. Quantifying genetic (co)variation and effects of genetic selection on tibial bone morphology and quality in 37 lines of broiler, layer and traditional chickens. *Br Poult Sci* 2009;50:443-450.
15. Corr SA, Bennett D, McCorquodale CC, et al. The effect of morphology on the musculoskeletal system of the modern broiler. *Anim Welf* 2003;12:145-157.
16. Frost HM. Why do marathon runners have less bone than weight lifters? A vital-biomechanical view and explanation. *Bone* 1997;20:183-189.

17. Albers GAA, Groot IA. Future trends in poultry breeding. *World Poult* 1998;14:42-43.
18. Wise DR. Skeletal abnormalities in table poultry - A review. *Avian Pathol* 1975;4:1.
19. Cook ME. Skeletal deformities and their causes: introduction. *Poult Sci* 2000;79:982-984.
20. Grist A. Poultry inspection: anatomy, physiology, and disease conditions. 2nd ed. Nottingham, U.K.: Nottingham University Press, 2006.
21. Jones RC, Kibenge FSB. Reovirus-induced tenosynovitis in chickens: the effect of breed. *Avian Pathol* 1984;13:511-528.
22. Kibenge FSB, Pass DA, Wilcox GE, et al. Bacterial and viral agents associated with tenosynovitis in broiler breeders in western Australia. *Avian Pathol* 1982;11:351-359.
23. Crespo R, Shivaprasad HL. Rupture of gastrocnemius tendon in broiler breeder hens. *Avian Dis* 2011;55:495-498.
24. Dinev I. Clinical and morphological studies on spontaneous rupture of the gastrocnemius tendon in broiler breeders. *Br Poult Sci* 2008;49:7-11.
25. Su G, Sørensen P, Kestin SC. Meal feeding is more effective than early feed restriction at reducing the prevalence of leg weakness in broiler chickens. *Poult Sci* 1999;78:949-955.
26. Danbury TC, Weeks CA, Waterman-Pearson AE, et al. Self-selection of the analgesic drug carprofen by lame broiler chickens. *Vet Rec* 2000;146:307-311.
27. Weeks CA, Grang A, Denton-Clark N, et al. Effect of leg weakness on behaviour of broiler chickens following food withdrawal. *Br Poult Sci* 1998;39:S8.
28. Sullivan TW. Skeletal problems in poultry: estimated annual cost and descriptions. *Poult Sci* 1994;73:879-882.
29. Varadarajan KM, Harry RE, Johnson T, et al. Can in vitro systems capture the characteristic differences between the flexion-extension kinematics of the healthy and TKA knee? *Med Eng Phys* 2009;31:899-906.
30. Fregly BJ, Rahman HA, Banks SA. Theoretical accuracy of model-based shape matching for measuring natural knee kinematics with single-plane fluoroscopy. *J Biomech* 2005:692.
31. Zavatsky AB. A kinematic-freedom analysis of a flexed-knee-stance testing rig. *J Biomech* 1997;30:277-280.
32. Bellemans J, Robijns F, Duerinckx J, et al. The influence of tibial slope on maximal flexion after total knee arthroplasty. *Knee Surg Sports Traumatol Arthrosc* 2005;13:193-196.
33. Ostermeier S, Hurschler C, Windhagen H, et al. In vitro investigation of the influence of tibial slope on quadriceps extension force after total knee arthroplasty. *Knee Surg Sports Traumatol Arthrosc* 2006;14:934-939.
34. Yildirim G, Walker PS, Boyer J. Total knees designed for normal kinematics evaluated in an up-and-down crouching machine. *J Orthop Res* 2009;27:1022-1027.

35. Kondo E, Merican AM, Yasuda K, et al. Biomechanical Comparisons of Knee Stability After Anterior Cruciate Ligament Reconstruction Between 2 Clinically Available Transtibial Procedures. *Am J Sports Med* 2010;38:1349-1358.
36. Howie RN: Biomechanical analysis of the effects of a total knee replacement on a canine stifle. MS: University of Georgia, 2011.
37. Wilson DR, Feikes JD, Zavatsky AB, et al. The components of passive knee movement are coupled to flexion angle. *J Biomech* 2000;33:465-473.
38. Fu Y-C, Torres BT, Budsberg SC. Evaluation of a three-dimensional kinematic model for canine gait analysis. *Am J Vet Res* 2010;71:1118-1122.
39. Series Displacement Sensors: Microminiature DVRT. Displacement Sensors: Microminiature DVRT. Available at: <http://www.microstrain.com/displacement/dvrt>. Accessed August 7, 2012.
40. Fleming BC, Beynnon BD. In Vivo Measurement of Ligament/Tendon Strains and Forces: A Review. *Ann Biomed Eng* 2004;32:318.
41. Lister SA, Renberg WC, Roush JK. Efficacy of immobilization of the tarsal joint to alleviate strain on the common calcaneal tendon in dogs. *Am J Vet Res* 2009;70:134-140.

## CHAPTER 4

### SUMMARY & CONCLUSION

#### 4.1 Summary

The previous two chapters described the 3-D kinematics of a normal canine and chicken stifle. The purpose of both studies was to characterize the normal stifle kinematics to use a basis of comparison after treatments were applied or among breeds. Both studies used a modified Oxford knee rig that preserved the hip and hock joints as well as the surrounding musculature to simulate flexion and extension. Kinematics were continuously measured and compared between treatments. Strain to the collateral ligaments in the canine as well as the gastrocnemius tendon in the broiler chicken were measured as well. Significant differences were detectable between kinematics and ligament strain in both the canine and broiler stifle, and results showed that the modified Oxford knee rig paired with a 3-D motion capture system may be used to investigate variables in the stifle *in vitro*. The large standard deviations in both studies indicate that a larger sample size is needed to accurately describe the kinematics of the stifle *in vitro*.

Results from the canine study suggest that the steepest tibial plateau angle restored the kinematics closest to those of the normal stifle. TKR with decreased plateau angles negatively affected adduction, internal rotation, and lateral translation. TKR at all plateau angles significantly decreased strain to the collateral ligaments, therefore TKR is not likely to cause damage to the collaterals unless the joint is severely over stuffed. The system used herein was not able to detect significant differences between a normal and CrCL deficient stifle as it did not simulate weight bearing, when the cruciate ligaments are strained.

Results from the broiler study suggest that there are quantifiable differences in kinematics between breeds with varying susceptibilities to leg deformities caused by genetic selection for rapid growth rate. The Athens-Canadian represents a traditional, random-bred chicken and showed stifle kinematics similar to results from *in vitro* human knees flexed passively. The 1996 Broiler and Commercial Broiler were both selected to represent breeds that have been bred for rapid growth to varying degrees. These breeds showed deviation from the random-bred chicken in abduction, internal rotation, and medial translation and also showed significantly greater strain to the gastroc tendon. The shorter tibiae and femurs of the faster growing breeds along with the significantly steeper tibial plateau angle of the Commercial Broiler suggest that bone length and plateau angle are also correlated with incidence of leg problems. Further investigation is needed to determine if there is a direct correlation between tibial plateau angle and abnormal stifle kinematics. Overall, results support the conclusion that genetic selection for rapid growth rate inhibits bone development and negatively affects broiler stifle kinematics.

#### 4.2 Future Recommendations

The results from these studies provide a basis for the characterization of abnormal kinematics within the canine stifle after TKR at varying plateau angles and the broiler stifle among breeds. The results herein may lead future research to optimize TKR and decrease the prevalence of leg problems in the broiler industry. To properly address the issues at hand with future studies, the following approaches may be helpful.

##### Canine Total Knee Replacement

- A characterization of stifle kinematics before and after TKR throughout a natural gait cycle, both *in vitro* and *in vivo* with greater sample sizes.

- A modified Oxford knee rig that simulates weight bearing as well as muscle pulls to more accurately mimic *in vivo* conditions.
- An investigation of steeper tibial plateau angles to determine at what angle kinematics no longer replicate those of the normal stifle.
- A characterization of contact pressure between the articulating surfaces of the TKR implant.

#### Broiler Chicken Stifle Kinematics

- A characterization of stifle kinematics among breeds throughout a natural gait cycle, both *in vitro* and *in vivo* with greater sample sizes.
- A modified Oxford knee rig that simulates weight bearing as well as muscle pulls to more accurately mimic *in vivo* conditions.